Universidade de Aveiro Departamento de Química
2007

Fatima Rodrigues Varanda

Medição de Equilíbrio Líquido-Líquido de Sistemas Bifásicos Fluorados

Measurement of Liquid-Liquid Equilibrium of Fluorous Biphasic Systems

Universidade de Aveiro Departamento de Química
2007

Fatima Rodrigues Varanda

Medição de Equilíbrio Líquido-Líquido de Sistemas Bifásicos Fluorados

Measurement of Liquid-Liquid Equilibrium of Fluorous Biphasic Systems

Dissertação apresentada à Universidade de Aveiro para cumprimento dos requisitos necessários à obtenção do grau de Mestre em Engenharia Química, realizada sob a orientação científica da Dra. Isabel Maria Delgado Jana Marrucho Ferreira, Professora Auxiliar do Departamento de Química da Universidade de Aveiro e do Dr. João Manuel da Costa e Araújo Pereira Coutinho, Professor Associado com Agregação do Departamento de Química da Universidade de Aveiro.

Aos meus pais, irmã e Pedro.

“Fundamental é mesmo o amor
É impossível ser feliz sozinho”
Tom Jobim (Wave)

o júri

presidente

Prof. Dr. Dmitry Victorovitch Evtyugin
Professor associado com agregação do Departamento de Química da Universidade de Aveiro

Prof. Dr. João Manuel da Costa e Araújo Pereira Coutinho
Professor associado com agregação do Departamento de Química da Universidade de Aveiro

Prof. Dra. Isabel Maria Delgado Jana Marrucho Ferreira
Professor auxiliar do Departamento de Química da Universidade de Aveiro

Dra. Ana Maria Antunes Dias
Estagiária de Pós doutoramento no Instituto de Biotecnologia e Bioengenharia da Universidade do Minho

agradecimentos

Em primeiro lugar quero agradecer à prof. Dra. Isabel Marrucho, por concordar em ser minha orientadora num momento que precisava de apoio e compreensão. Além disso, foi de extrema importância na parte final da execução dessa dissertação, ao corrigir exaustivamente o que escrevi. Ao prof. Dr. João Coutinho agradeço também por me perguntar todos os dias se eu já tinha um sistema novo medido. Pude assim ver que determinados trabalhos experimentais são só para aqueles que têm paciência. Por incrível que pareça, isso me fez acreditar mais em mim, nas minhas capacidades.

A todos os membros do grupo PATh (Ana Caço, Ana Dias, Carla, Fátima Mirante, Mara, Maria Jorge, Mariana Belo, Mariana Costa, Nelson, Nuno, Pedro, Ramesh, Sónia, Tozé e meninas dos Projectos) o meu MUITO OBRIGADA. É uma pena pensar que não existem muitos locais de trabalho tão divertidos! Mas é reconfortante saber que pude partilhar isso com vocês. Tenho certeza que nunca vou esquecer vocês!

Dentro desse grupo tenho que destacar algumas pessoas. A Maria Jorge esteve sempre ao meu lado, vendo e revendo os meus pontos (“Será que já turvou? Olha só os resultados! Nunca mais turva, quer dar uma voltinha?”). Acho que tudo o que fiz passou por ela. Não tenho palavras para agradecer tudo o que fez por mim! A Mariana Costa, a Ana Dias, o Nuno, o Pedro e a Mara são aqueles que aos fins de semana, durante noites divertidíssimas que acabavam sempre com “discussões” de trabalho, me ensinaram e deram muitas dicas. A Ana Caço ajudou todas as vezes que necessitava de um material ou de um cafezinho de manhã.

Provavelmente não teria feito este mestrado sem meus pais, que me apoiaram em toda minha vida e não hesitaram em me dizer que eu deveria concorrer. A minha mãe teve que me aturar durante esses 10 meses contando cada pormenor das experiências e de tudo o que acontecia todo santo dia. O meu pai, apesar de ter estado do outro lado do Atlântico durante a maior parte deste tempo, esteve sempre preocupado e perguntava sempre, por telefone, como tudo estava correndo. Agradeço ainda à minha irmã, que esteve sempre despreocupada, pois sabia que eu era capaz. Ao meu namorado Pedro nem sei como agradecer. Durante esses anos todos de convivência tem sido quem me apoia, me ajuda e me acorda para a realidade à minha volta.

MUITO OBRIGADA, a todos vocês e a todos os outros que se cruzaram comigo. Todos contribuíram de alguma maneira. Tenho certeza de que apesar de ter sido um curto período, aprendi muito, não só sobre o tema dessa dissertação, mas sobre a vida, sobre a convivência, sobre a amizade.

palavras-chave

catálise bifásica, perfluorocarbonetos, equilíbrio líquido-líquido, experimental, COSMO-RS, soft-SAFT.

resumo

A catálise heterogénea é usada em 80% dos processos industriais catalíticos porque envolve uma fácil separação dos reagentes e produtos da reacção. A catálise homogénea, por sua vez, apresenta a grande vantagem de se poder usar diversos modelos capazes de descrever e prever as propriedades da mistura reaccional, embora apresente uma difícil separação e recuperação dos compostos envolvidos. A catálise bifásica consegue reunir as vantagens de ambos os tipos de catálise homogénea e heterogénea. Este método consiste em utilizar dois solventes imiscíveis a temperatura ambiente, onde o catalisador encontra-se imobilizado em uma fase e os reagentes na outra. Através de um aumento da temperatura forma-se uma única fase onde ocorre a reacção. Ao arrefecer, as fases separam-se permitindo a separação dos produtos e do catalizador, que pode ser reutilizado. Em particular, desde a primeira publicação, em 1994, que Horváth e Rábai demonstraram que os sistemas bifásicos fluorados podem ser altamente vantajosos em uma grande variedade de reacções químicas orgânicas, usando perfluorocarbonetos como meio de reacção.

Este trabalho tem como principal objectivo o estudo do equilíbrio líquido-líquido de sete novos sistemas binários contendo compostos fluorados e solventes orgânicos, contribuindo com novos dados experimentais e teste de modelos nestes sistemas. O método utilizado foi a turbidimetria, usando um método dinâmico de detecção visual. Foram preparadas várias ampolas com composições diferentes para cada sistema. A mistura foi aquecida em um banho termostatizado a uma temperatura onde apenas uma fase era observada. Ao arrefecer lentamente essa mistura, observou-se a separação das fases e a respectiva temperatura foi registada.

Os resultados obtidos foram correlacionados coma dois modelos que usam diferentes abordagens. A equação de estado soft-SAFT foi utilizada para correlacionar os dados experimentais de forma satisfatória. O COSMO-RS, modelo baseado em cálculos de química quântica foi utilizado para prever o comportamento das solubilidades mútuas dos compostos envolvidos, tendo-se verificado uma ferramenta útil no caso de sistemas envolvendo tolueno e acetonitrilo.

keywords FBS; PFC; Liquid-liquid equilibrium; experimental; COSMO-RS; soft-SAFT

abstract

Due to the easy separation of the reactants from reaction products, almost 80% of industrial catalytic reactions use heterogeneous catalysts. The homogeneous catalysis has the great advantage that models can be used to describe and predict the properties of the species involved in the catalytic reaction, but its main limitation is the separation and recovery of the products from the catalyst. The biphasic catalysis gather the advantages of both types of catalysis. This method consists on using two solvents which are immiscible at room temperature maintaining the catalytic system immobilized in one phase while the reactants and products remain in the other phase. By rising the temperature, the mixture becomes completely miscible allowing reactions to proceed homogeneously. On cooling, the phases separate allowing the facile catalyst/product separation. Since the first publication in 1994, by Horváth and Rábai, fluorous biphasic systems (FBS) have shown to have advantages in a wide variety of chemical organic reactions including catalytic reactions, using perfluorocarbons (PFC) as reaction media.

The aim of this work is the study of liquid-liquid equilibrium (LLE) of seven original binary systems containing highly fluorinated compounds and an organic solvent. This work contributes with new experimental LLE data of fluorous biphasic systems, measured using turbidimetry with naked eye visual detection. Several ampoules were prepared with different compositions for each system. The mixture was heated in a thermostatic bath until just one phase was observed. On slowly cooling, the phase separation temperature was registered.

The obtained results were modeled using two different approaches. The soft-SAFT equation of state was used successfully to correlate the experimental data. COSMO-RS, a predictive method based on unimolecular quantum chemical calculations for individual molecules, was used to predict the phase behavior of the involved compounds and revealed to be a special useful tool in the case of toluene and acetonitrile mixtures.

Index

List of Figures

List of Tables

List of symbols

Roman letters and abbreviations

A	Total surface area (Chapter 4.1); Helmholtz free energy (Chapter 4.2)
a	Contact area between two surface segments
AAD	Average absolute deviation
c	Coefficient (for hydrogen bond strength, Chapter 4.1)
E	Energy
EoS	Equation of State
FBS	Fluorous Biphasic System
FC	Fluorocarbon
HC	Hydrocarbon
LJ	Lennard-Jones
LLE	Liquid-Liquid Equilibrium
m	Chain length (for Lennard-Jones segments)
M	Molecular weight
p	Order parameter (Chapter 3.1); Profile (Chapter 4.1)
PFC	Perfluorocarbon
PFMCH	Perfluoromethylcyclohexane
Q	Quadrupolar moment
RG	Renormalization Group
SAFT	Statistical Associating Fluid Theory
SLE	Solid-Liquid Equilibrium
T	Temperature
UCST	Upper Critical Solution Temperature
w	Weight fraction
x	Mole fraction
X	Molecule considered as solute

List of Greek letters

τ	Reduced temperature (Chapter 3); Element-specific vdWs coefficient (Chapter 4.1)
φ	Volume fraction
α	Critical exponent
α'	Electrostatic misfit interactions coefficient
β	Critical exponent
ε	Segment interaction energy (between Lennard-Jones segments)
η	Size parameter of the generalized Lorentz-Berthelot combination rules
ξ	Energy parameter of the generalized Lorentz-Berthelot combination rules
ρ	Mass density ($kg.m^{-3}$)
σ	Polarization charge density (Chapter 4.1); Size parameter of the intermolecular potential/diameter (for Lennard-Jones segments) (Chapter 4.2)

List of indices

assoc	Association term for soft-SAFT EoS
c	Critical
chain	Chain term for soft-SAFT EoS
eff	Effective
HB	Hydrogen bond
i	Component
polar	Polar term for soft-SAFT EoS
ref	Reference term for soft-SAFT EoS
S	Solvent
vdW	van der Waals

“It is ironic that organic synthesis and separation science are separate disciplines because synthesis and separation are inseparable.”

Dennis Curran

1 INTRODUCTION

The study of catalysis is a fundamental theme in the development of the chemical industry, since more than 80 % of chemical products are obtained by processes that need a catalyst in, at least, one of the steps of the mechanism. Currently, almost 80 % of industrial catalytic reactions use heterogeneous catalysts,[1] although during the second half of 20th century, the interest in homogeneous catalysis increased in parallel with the development of organometallic chemistry.

The main advantage of heterogeneous catalysis is the easy separation of the catalyst and/or the exhausted reagents from the products of reaction. However, homogeneous catalysis has a great potential, as molecular models can be used to accurately predict the properties of the catalytic species.[2] It also allows a better understanding of the reactions mechanism at the molecular scale, making the optimization of some homogeneous catalytic industrial processes, such as the carbonation of methanol for acetic acid synthesis (Monsanto process), olefins oligomerization (SHOP process) or hydroformylation of propene (oxo process),[3] an easier and feasible task. The main limitation of the application of homogeneous catalysis at the industrial scale is the separation of the products from the catalyst and its recovery on a sufficiently large amount in its activated form. This separation is generally obtained by distillation, that can cause products degradation, or by polymerization of part of products into heavier compounds that will remain in the catalytic phase and can cause the inactivation of catalyst. Another way of separating the reaction products from the catalyst consists on submitting the catalyst to a sequence of chemical modification and extractions, with a substantial loss of metal.

Up to the present, the most efficient way to avoid these problems and to use homogeneous catalysis in many industrial processes is the so-called biphase catalysis. This method consists on using two immiscible solvents, maintaining the catalytic system immobilized in one phase (polar organic, fluorous, ionic liquid or aqueous) while the reactants and products remain in the other phase (usually an organic solvent). By simple decantation, both phases are easily separated and the

catalytic system can be recycled. Since both phases are non miscible, the reaction takes place at the interface and/or inside the catalytic phase, usually needing vigorous stirring.

Nowadays, there are many examples of biphasic systems that are applied in different homogeneous catalytic processes. Among them, fluorous biphasic systems (FBS) deserve a special mention. They consist of a fluorous phase, normally a perfluorocarbon (PFC) solvent containing a dissolved catalyst and a second organic or aqueous phase, containing a dissolved substrate, which has limited solubility in the fluorous phase.[4-6] This kind of system is based in the concept of thermo-dependence miscibility of fluorous solvents in organic compounds.[7] The advantage of the FBS is that certain mixtures of organic and fluorinated carbon (FCs) solvents become completely miscible at high temperatures allowing reactions to proceed homogeneously with a maximum contact with catalyst and reactants. On cooling, the phases separate allowing the facile catalyst/product separation (Figure 1.1).

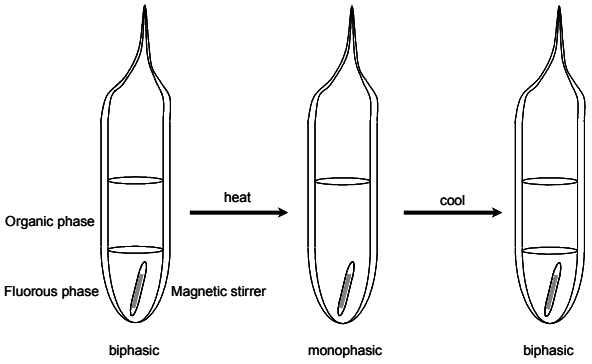

Figure 1.1. Scheme of thermo-dependence miscibility of fluorous solvents and organic compounds.

The fact that fluorous solvents are considered non-toxic, provides to FBS the label of environmentally friendly solvent according to the Green Chemistry regime. Therefore, FBS attract a high interest in a wide variety of industrial processes, such as the catalytic production of organic compounds.

Two scenarios can be distinguished in FBS concept: the first one occurs at room temperature in a heterogeneous medium where the reaction takes place at the interface of the two liquids; in the other, the reaction takes place in a homogeneous medium by rising the temperature.

This concept has become so popular that FBS kits are commercially available to perform some of the basic catalyzed organic reactions, such as hydroformylation of alkenes,[7] hydrogenation,[8] hydride reduction,[9] hydroboration,[10] oxidation,[5, 11] and oligomerization of olefins.[12] In Table 1.1, the list of the most representative FBS in use are presented and details are following described.

Table 1.1. Most representative FBS solvents.

Fluorocarbon	**Organic/aqueous solvent**	**Application**
perfluoromethylcyclohexane	toluene	Living Radical polymerization; Hydroformylation of olefins; Hydroboration
perfluoro-*n*-octylbromide	toluene	Cross-coupling reactions; Oxidation of sulfides and olefins
perfluoroether	toluene	Oligomerization of ethylene
perfluorodecalin	toluene	Oxidation of aldehydes, olefins and sulfides; Transesterification
perfluoroether	alkane	Oxidation of cyclohexane
perfluorohexane	acetonitrile	Photooxidation of allyl alcohols; Epoxidation of olefins
perfluoromethylcyclohexane	1,2-dichloroethane	Esterification of carboxylic acid; Baeyer-Villinger oxidation
perfluoro-*n*-octylbromide	benzene	Wacker oxidation
perfluorobutyltetrahydrofuran	*p*-toluenesulfonic acid	Synthesis of carboxylic ester

Hydroformylation[7, 13, 14]

The first publication that showed the great potential of FBS[7] focused on the hydroformylation of 1-alkenes. At room temperature, 1-alkenes are soluble in toluene while the catalyst, $[\{(CF_3(CF_2)_5CH_2CH_2P_3\}_3(CO)RhH]$, is soluble in perfluoromethylcyclohexane (PFMCH). This reaction is conducted at 100 ºC, when both toluene and PFMCH form one homogeneous phase, in the presence of CO/H_2. Once the mixture is cooled down to room temperature, the separation of reaction products (aldehydes) from the catalyst occurs, since the two solvents used become immiscible.

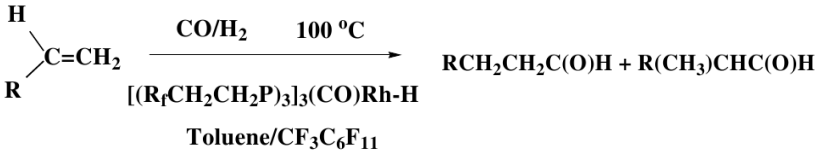

Hydrogenation[8]

The hydrogenation of organic compounds with transition metal hydrides is another example of FBS applications. An aliphatic version of Wilkinson's catalyst was modified with fluoroponytails in order to make it soluble in PFMCH. The reaction is carried out with H_2 at 1 atm and 45 ºC under heterogeneous conditions, providing cyclododecane with 94 % yield. The fluorous phase containing the catalyst is recycled allowing several runs.

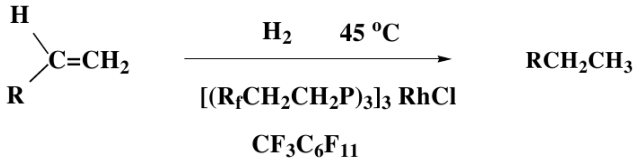

Hydride reduction[9]

Another interesting FBS example was reported using $[\{CF_3(CF_2)_5CH_2CH_2\}_3SnH]$ as a catalyst, that can be used in various free-radical reduction reactions with trifluoromethylbenzene as solvent. Adding a reducing agent, $NaCNBH_3$, this process can be made catalytic to recycle the SnH from SnX,

while separation of the fluoroponytailed organotin halide from the reduced product for recycling was accomplished by a fluorocarbon extraction procedure.

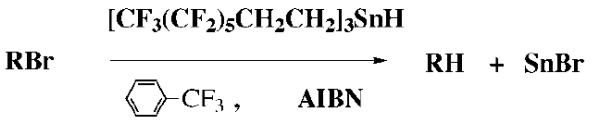

Hydroboration[10]

The FBS process can be used for the facile separation of the fluoroponytailed catalyst from products is the classical hydroboration reaction. Using the aliphatic Wilkinson's catalyst, with catecholborane and an alkene, hydroboration occurs providing a compound, that is oxidized by H_2O_2 directly to alcohol (next step) and the fluorous phase containing the catalyst is recycled.

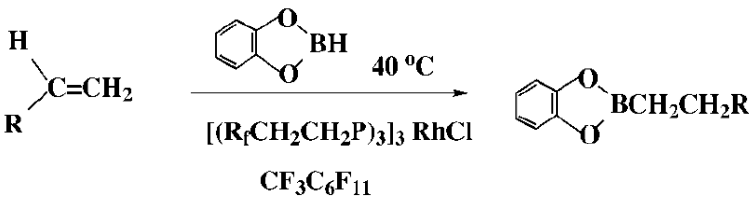

Alkene epoxidation[15]

PFCs are good solvents for gases and so FBS can be a good choice for performing classical oxidation reactions, such as, epoxidation or alkane/alkene functionalization. An example of a fluoroponytailed non-porphyrin Ruthenium complex is shown in the FBS epoxidation of disubstituted olefins at 50 ºC.

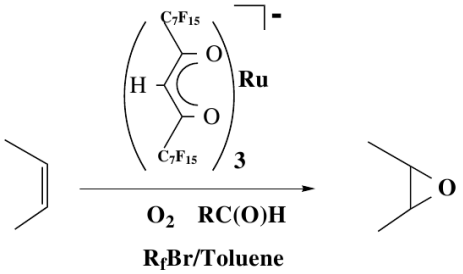

Alkane and alkene functionalization[11]

The functionalization of alkanes and alkenes to alcohols, aldehydes and ketones under FBS oxidation conditions represents an important advance for the catalytic synthesis of globally important organic chemicals. As usual, recycling the fluorous phase permits a continuous oxidation process, but further research to develop a possible industrial scenario is still needed.

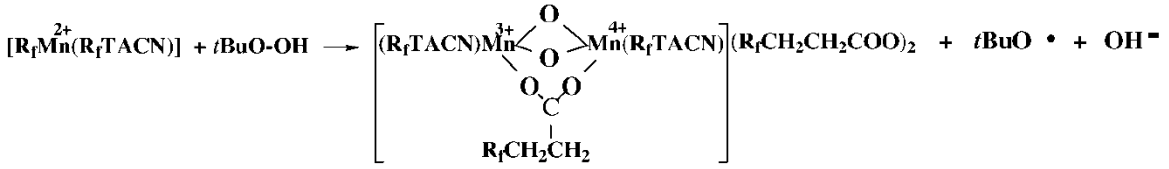

The FBS characteristics and feasibility are mainly due to the unique characteristics exhibited by perfluorinated compounds. The FCs are synthetic compounds defined as saturated fluids, like alkanes, alkenes, ethers or amines, in which the hydrogen atoms are partially or completely substituted by fluorine atoms.[14] When all of hydrogen atoms are substituted by fluorine atoms these compounds are called perfluorocarbons. PFCs present physical and chemical properties quite different from their corresponding hydrogenated compounds. They have strong intramolecular forces (C-F bond dissociation energy ~ 116 kcal.mol^{-1} while C-H bond dissociation energy is ~ 99 kcal.mol^{-1})[16] and very weak intermolecular forces, due to fluorine's high ionization potential. These two factors are the main responsible for the interesting properties presented by perfluoroalkanes when compared with the corresponding hydrocarbons (HCs), as for example:

- higher solubility for gases (the highest known among organic liquids);
- exceptional chemical and biological inertness;
- excellent spreading characteristics and higher fluidity;
- lower surface tensions;

- lower refractive indices (lower than 1.3);
- higher vapor pressures;
- higher densities;
- higher viscosities;
- higher isothermal compressibilities;
- lower internal pressures;
- poorer solvency for organics;
- non-polar molecules;
- nearly ideal liquids.

In Table 1.2 the values of some of the relevant properties are listed for the PFCs, together with the organic compounds, used in this work.

Table 1.2. Physicochemical properties of the compounds studied in this work.

Compound	**Molar weight /** g.mol^{-1}	**Mass Density [a]/** kg.m^{-3}	**Vapor pressure [a]/** kPa	**Boiling point /** K	**Polar Interactions**
perfluorodecalin	462.08	1.9305 [17]	0.936 [17]	415.17 [17]	
perfluoromethylcyclohexane	350.05	1.7880 [18]	14.105 [19]	349.30 [19]	
perfluoro-*n*-octane	438.06	1.7647 [20]	3.765 [20]	377.36 [21]	
1Br-perfluoro-*n*-octane	498.97	1.9148 [17]	0.722 [17]	416.11 [17]	
1H-perfluoro-*n*-octane	420.07	1.7499 [17]	2.133 [17]	385.48 [17]	
1H,8H-perfluoro-*n*-octane	402.08	1.7534 [22]	1.019 [22]	399.43 [21]	
toluene	92.14	0.87	5.277 [19]	383.8 [19]	- 8.00 [23][b]
					1.25 x10^{-30} [24][c]
acetonitrile	41.05	0.782	11.795 [19]	354.8 [19]	13.08 x10^{-30} [19][c]
n-octane	114.23	0.702	1.863 [19]	398.7 [19]	

[a] densities and vapor pressures at 298.15 K; [b] quadrupole moment (Buckingham); [c] dipole moment (C.m)

Although PFCs have a high capacity to solubilize gases like carbon dioxide, oxygen, nitrogen, hydrogen and helium,[20,22] they do not mix with common solvents and water due to their extremely high hydrophobicity.[25] When PFCs are mixed

with non-fluorine solvents, the deviations from ideality are positive and larger than those of nearly all other classes of mixtures containing only non-polar and non-electrolyte substances. The most noticeable consequences of the extent of these deviations are the marked positive azeotropy (double azeotrope can even be observed in the perfluorobenzene + benzene system) and liquid-liquid immiscibility[26] and also in surface properties, negative aneotropy or surface azeotropy.[27] Differences in chain flexibility of the two component molecules and the weak interaction energy interplay are most probably the main responsible for the occurrence of these phenomena.[28]

There are three main areas where the use of perfluorocarbons present substantial advantages: biomedical, industrial and environmental.

Due to their great capacity to solubilize gases, PFCs are used for biomedical purposes. The main application of pure PFCs is in liquid ventilation[29] and in emulsified form as potential red cell blood substitutes. Other applications in clinic specializations include the cardiovascular,[30, 31] oncology[32] and organ-preservation[33] fields that are currently under investigation. PFCs are considered in all the situations of surgical anemia, some haemolytic anemias, ischemic disease, angioplasty, extracorporeal organ perfusion, cardioplegia,[34] radiotherapy of tumours[35] and as an ultrasound contrast agent to detect myocardial perfusion abnormalities.[36]

Concerning industrial purposes, there are a large number of documented applications regarding perfluoroalkanes. PFCs can be used as co-solvents in supercritical extraction, improving the solubility of hydrophilic substances in supercritical reaction or extraction media.[37] Short-chain halocarbons are used as refrigerants, aerosol propellants and foam blowing agents. These compounds can also be used in cell culture aeration, as was recently presented in an interesting PhD thesis by Freire.[38] Finally, as medium in two-phase reaction mixture, as it was described above.

Due to the exceptional solubility of carbon dioxide in perfluoroalkanes these compounds are being studied for industrial and environmental applications as the

removal of carbon dioxide from gaseous effluents.[39]

Despite the enormous potential that PFCs have in their application to the biomedical field, finding one PFC that fulfills all the pre-requisites is sometimes an almost impossible task. In order to fulfill the desired specifications, an easy way is to use a formulation of PFCs so that the desired properties can be tailored according to the purposed. Thus, the study of the impact that these small structural variations have in the desired thermophysical properties is of great importance. There are some studies already published in the literature on PFCs + HCs phase equilibria which clearly show how this type of system can capture small changes in structure. In this work, some time will be dedicated to the study of phase equilibria of binary systems containing *n*-octane + perfluoro-*n*-octane derivatives.

1.1 Motivation

Despite the great number of possible applications for these compounds, data for fluorocarbons is old, discrepant, incomplete and/or, in some cases, non existent. For example, regarding liquid-liquid equilibrium (LLE) data of systems involving these compounds it is very common that just the phase separation temperature for an equivolume mixture is reported. This is only justified by the fact that the phase equilibrium diagram is usually symmetric, when temperature is plotted as a function of volume fraction (φ), with the upper critical solution temperature (UCST) approximately at φ = 0.5. From now on, the UCST will just be called T_c, for simplicity.

The importance of having a wide thermophysical database on these compounds which possess unusual properties is enormous since most of the correlation and prediction models usually used in engineering present large deviations for these systems. The understanding of their peculiar behavior is thus crucial in order to develop accurate models which will allow the prediction of the relevant thermophysical properties regarding the application of these compounds at the temperature and pressure of interest. In that context, this dissertation is another contribution in the effort devoted to the characterization of perfluoroalkanes and their mixtures. The main objective is to complement/validate experimental data available in the literature, to present accurate original experimental data that, besides the practical direct interest, can help to answer/validate the theories and models related to highly fluorinated systems.

This thesis is divided in 2 parts: an experimental part where LLE of the systems with interest in FBS (perfluorodecalin + toluene, perfluoromethylcyclohexane + toluene, perfluorodecalin + acetonitrile, perfluoromethylcyclohexane + acetonitrile and 1Br-perfluoro-*n*-octane + acetonitrile) and substituted fluorocarbons (1Br-perfluoro-*n*-octane, 1H-perfluoro-*n*-octane and 1H,8H-perfluoro-*n*-octane) + *n*-octane were measured by turbidimetry using the dynamic visual detection method; and a second part where

two models based on different approaches were used to correlate and predict the experimental data measured.

In Chapter 2 the details for the validation of the method, the experimental setup and the data acquisition procedure used for the measurement of LLE data will be described. Original equilibria data on seven binary systems involving FCs will be reported in Chapter 3.

In Chapter 4, two different models will be described: an equation of state, soft-SAFT and the COSMO-RS, based on molecular quantum chemical calculations. A general introduction for each model will be made and the results obtained for each model will be compared with the experimental data.

The last chapter is reserved for the final conclusions and some thoughts for future work.

2 Materials and Methods

2.1 Materials

Liquid–liquid equilibria of binary mixtures of cyclic and substituted FCs + organic solvent were measured using a synthetic method, turbidimetry, at the vapor pressure of the mixture. All the solvents were used without any further purification except perfluorodecalin, that was purified by passage through a silica column (approximately 10 times).[40] Table 2.1 presents some information about each one of the compounds used in this work.

The purity of each FC was analyzed by GC with a Varian Gas Chromatograph CP 3800 with a flame ionization detector (FID). Chromatographic separations were accomplished with a Varian CP-Wax 52CB column with an internal diameter of 0.53 mm and equipped with Coating WCot Fused Silica.

Table 2.1. Formula, purity and supplier of the studied compounds in this work.

Compound	**Formula**	**Purity** (wt %)	**Supplier**	**CAS No.**
perfluorodecalin	$C_{10}F_{18}$	99.88	Flutec	306-94-5
perfluoromethylcyclohexane	C_7F_{14}	99.98	Apollo Scientific	355-02-2
perfluoro-*n*-octane	C_8F_{18}	98.36	Fluorochem	307-34-6
1Br-perfluoro-*n*-octane	$C_8F_{17}Br$	99.90	Apollo Scientific	423-55-2
1H-perfluoro-*n*-octane	$C_8F_{17}H$	97.05	Apollo Scientific	335-65-9
1H,8H-perfluoro-*n*-octane	$C_8F_{16}H_2$	99.10	Apollo Scientific	307-99-3
toluene	C_7H_8	99.5	Panreac	108-88-3
acetonitrile	CH_3CN	99.7	LabScan	75-05-8
n-octane	C_8H_{18}	99.5	Fluka	111-65-9

2.2 Methods

Generally, the experimental methods for determination of phase equilibrium can be divided in two categories: synthetic and analytical.[41] The choice for one particular method depends on many factors, such as stability of the compounds, desired accuracy, level of solubility, available instrumentation, etc... Probably the most important factor is the level of (mutual) solubility of the solvents, since it can vary from completely soluble under any condition to virtually non soluble.

The synthetic method involves the preparation of a mixture of known composition, generally in terms of mass, followed by the experimental determination of the temperature at which the phase separation occurs. Traditionally, this temperature is determined by visual observation, but methods using light dispersion can also be used.[42] In order to use visual observation the cloud points have to be easily detected, so that the phase diagram is obtained with good accuracy. If the components are stable, this method can be virtually applied to any liquid-liquid system. In addition, this method is very simple, not needing any costly equipment: an analytical balance, common glass laboratorial material and a heating device can be used with good results. The two major limitations are that it is not applicable to very low solubilities and the fact that it is very time consuming.

In the analytical method, two liquid phases are put in contact until they reach the equilibrium (mutual saturated). Then, both phases are separated, sampled and analyzed by an appropriated analytical quantitative method (usually, GC or HPLC).

In this work, the dynamic synthetic method was chosen since, besides being very simple to use, the systems chosen satisfy all the pre-requisites. The determination of the temperature cloud points was made by turbidimetry using naked eye inspection while the temperature is changed very slowly for a system with a fixed composition, so that the error inherent to the operator is reduced. The observations were performed at the vapor pressure of the system for that temperature. Since at low pressures (bellow 100 atm) the system pressure has usually a negligible effect in the liquid-liquid solubility,[42] the pressure effect on the

phase diagram was not taken into account in this work.

2.2.1 Experimental Procedure

Sample preparation:

All samples were prepared in glass ampoules containing a magnetic stirrer. The dimensions of the used ampoules were approximately 50 mm x 9.0 mm x 1.0 mm (height x extern diameter x thickness), which gives an approximate volume of 2.5 cm^3. Using a diagram of safe working pressures of the glass material used, an ampoule with a height of 500 mm (the smallest height considered in the diagram) can safely work until 14 atm of internal pressure.[43] As the smaller is the ampoule, the higher is the safe working pressure, all the calculations were made for the maximum temperature that could be reached for each mixture composition taking into account that the safe work pressure considered was 14 atm.

The ampoules described above containing a magnetic stirrer covered by glass inside were made in the Glass Workshop of University of Aveiro. Before the introduction of any compound, each ampoule was cleaned with nitric acid to ensure that the magnetic stirrer was well covered with glass. If that is not the case, the magnetic stirrer changed its color due to oxidation and the ampoule is rejected. Then, the ampoules were cleaned with distilled water and finally they were put in the oven at 140 ºC for 2 hours to allow the evaporation of any solvent residues still present.

Each compound was rigorously weighted using an analytical high precision balance (± 0.1 mg), with help of a syringe and a needle, and the respective weight, mole and volume fractions were determined. The fluorinated compound migrates to bottom of the ampoule due to its higher density.

The mixture inside the ampoules was immediately frozen in liquid nitrogen, avoiding any changing in composition and sealed under vacuum, in order to minimize the air content inside of the ampoule (Figure 2.1). For each system, 10 ampoules with different compositions were usually prepared.

Figure 2.1. Preparation of the ampoules used in this work.

Temperature Cloud Point Determination:

Each sample, with a different composition, was immersed in the thermostatic bath. The thermostatic fluid used was water for measurements between 303 K and 353 K and commercial vegetable oil for higher temperatures. The setup used to thermostatize the working mixture inside the ampoule consists on a sufficiently large glass beaker, which was placed on a hot plate, and a magnet was used to manually stir the sample mixture inside the ampoule, in order to ensure the homogeneity of the sample throughout the experience (Figure 2.2, left).

When the prepared mixture was homogeneous at room temperature or near

it, other experimental setup was mounted to heat/cool the ampoule. For temperatures between 263 K and 303 K, the ampoule was immersed in a jacketed cell of water with an anti-frozen liquid (ethylene glycol mono-ethyl ether 99 % pure, from Panreac) bath, using a JULABO F25 circulator (Figure 2.2, right). The same fluid circulates also inside the jacket of the cell.

In both setups, cloud point temperatures were obtained with a Pt100 temperature sensor connected to a digital multimeter (HP 974A, 5 digits with 2 decimal places). Before hand, this sensor was calibrated against a Platinum Resistance Thermometer (model 5613) with a thermometer Read Out (model 1521) from Fluke (Hart Scientific), which had been calibrated against a SPRT (25 ohm, Tinsley, 5187A) temperature probe using an ASL bridge model F26. The calibration curve is provided in Appendix A.

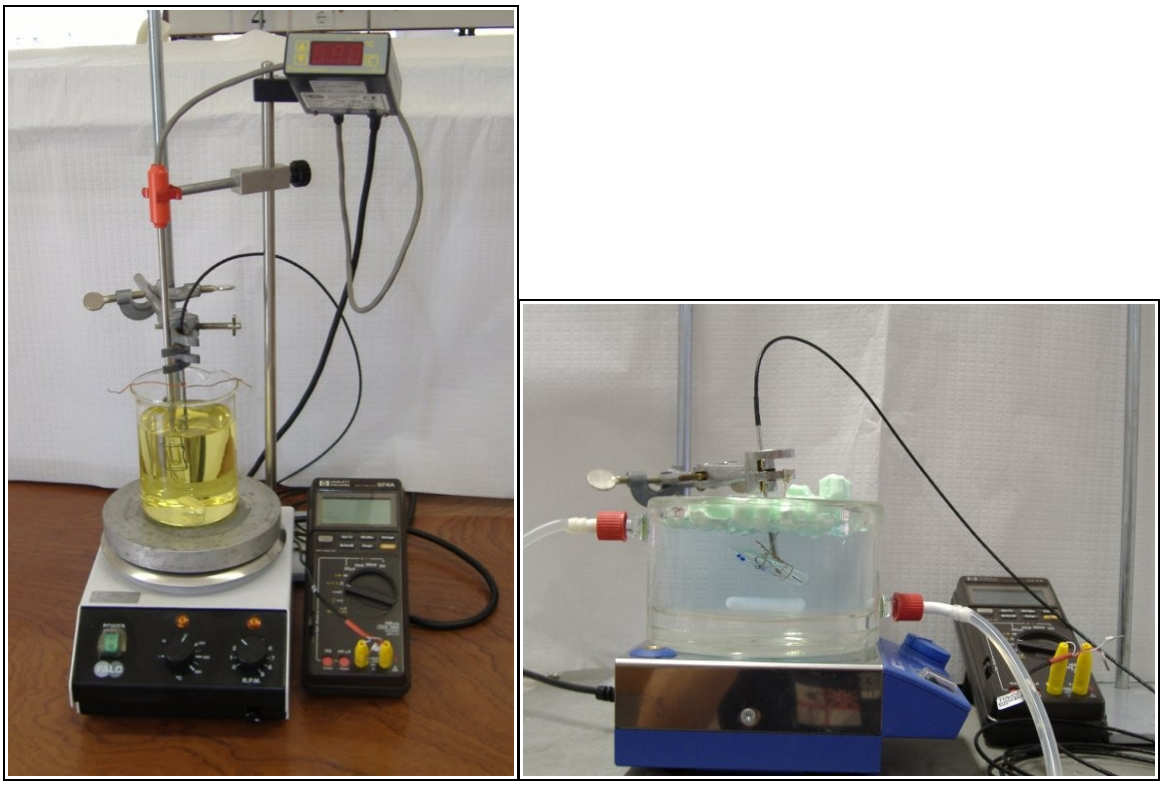

Figure 2.2. Experimental apparatus used for high (left) and low (right) temperatures.

The experimental procedure consisted on heating up the sample until just one phase was observed. During that time, the mixture was manually stirred, with the help of a magnet, so thermal equilibrium was faster obtained. Then, temperature was slowly cooled down (< -0.05 $K.min^{-1}$) so that the error in the cloud point temperature determination is minimized,[44] until phase separation was detected by visual observation (Figure 2.3). The resistance value of the Pt100 was taken and the procedure was repeated until three independent agreeing values were obtained.

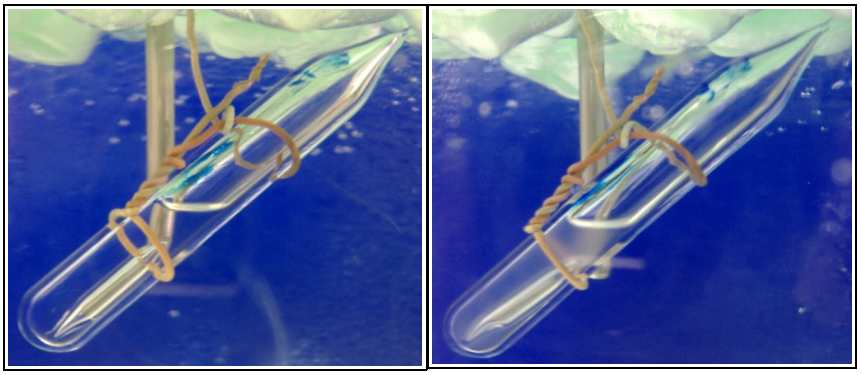

Figure 2.3. Ampoule with homogeneous (left) and heterogeneous (right) behavior.

3 Results and Discussion

3.1 Calibration

In order to evaluate the performance of the present setup in terms of accuracy and precision and also to get used to the visual determination of the cloud points of systems containing FCs, a well studied system, perfluoro-*n*-octane + *n*-octane, was measured. This system was used to calibrate the apparatus since it is similar to those of interest and there are data available in the open literature.[45] The results obtained are listed in Appendix B – Table B.1 and represented in Figures 3.1 and 3.2 together with literature data.[45]

Compositions, expressed in terms of volume fractions of fluorinated compound (φ_1), were calculated using the follow relation:

$$\varphi_i = \frac{x_i}{x_i + K(1 - x_i)} \qquad (1)$$

where $K = \frac{(\rho_i M_j)}{(\rho_j M_i)}$, and ρ and M are the mass density and the molecular weight, respectively, and the indices i and j indicate i and j components. The values of mass density used were taken from literature and are presented in Table 2.1.

As it can be observed, the data measurement are in good agreement with those presented by Melo et al.[45] when calculated in terms of mole or volume fractions. Note the symmetry of LLE line when the volume fraction representation is used (Figure 3.2). A systematic data representation was used in the Figures throughout this work as follows: filled symbols represent the measured data and each color represents always the same FC, non-filled symbols represent literature data, one symbol represents always the same organic solvent, the cross represents the T_c of each system determined by the renormalization group theory (see Chapter 3.2).

The experimental data measured for the PFMCH + toluene binary system is compared with literature data[13] in Figures 3.3 and 3.4. This system can also be used to test the performance of our experimental set up. Small deviations can be observed between the data measured within this work and literature data, being

the cloud point temperatures measured here systematically higher than those presented by Hildebrand and Cochran.[13] However, it is possible to give some justifications for them: in the cited article,[13] the authors do not state the purity of the perfluoroalkane; the compounds quantity was measured by volume, that incurs in larger errors than in terms of mass, as it was done in this work; and the ampoules were not prepared under vacuum, which avoids the presence of air inside of the ampoule, which can therefore oxidate the PFCs. Again, notice the symmetric behavior of the LLE line when the volume fraction representation is used (Figure 3.4). As for most systems, this kind of diagram for PFCs + HCs mixtures are more symmetric when represented in terms of volume fraction as compared to mole fraction.

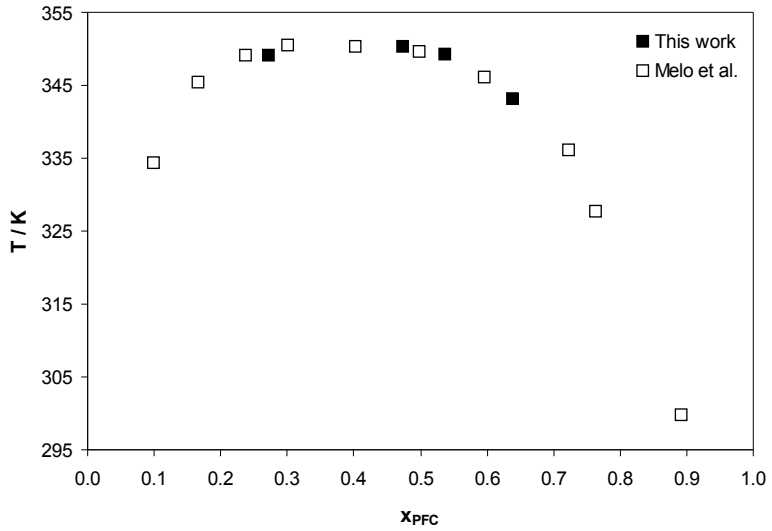

Figure 3.1. Experimental data of perfluoro-*n*-octane + *n*-octane system in terms of mole fraction. The non-filled symbol represent Melo et al. data.[45]

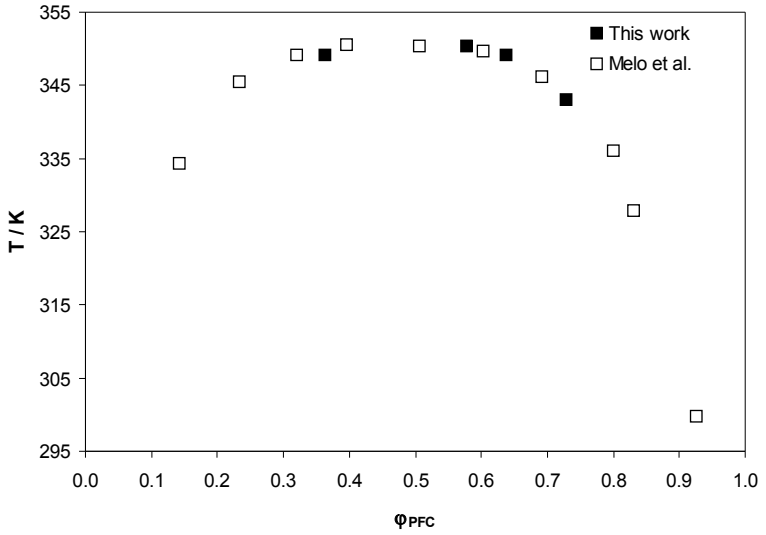

Figure 3.2. Experimental data of perfluoro-*n*-octane + *n*-octane system in terms of volume fraction. The non-filled symbol represent Melo et al. data.[45]

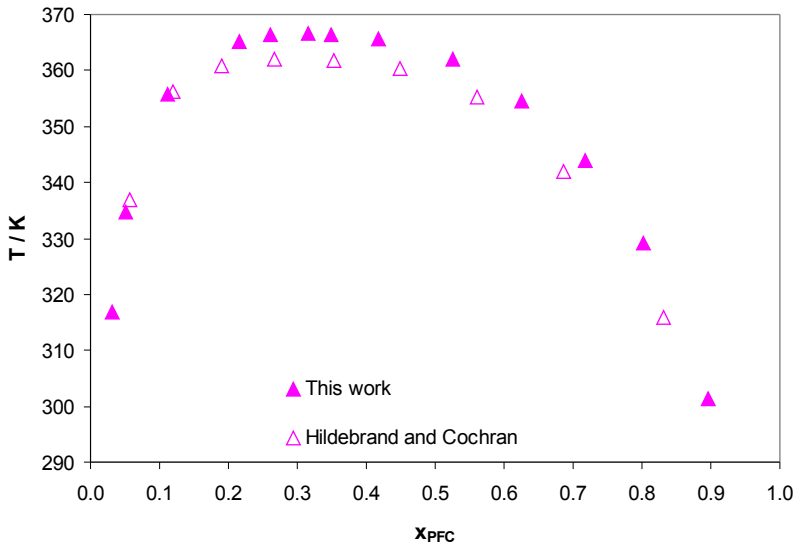

Figure 3.3. Experimental data of perfluoromethylcyclohexane + toluene system in terms of mole fraction. The non-filled symbol represent Hildebrand and Cochran data.[13]

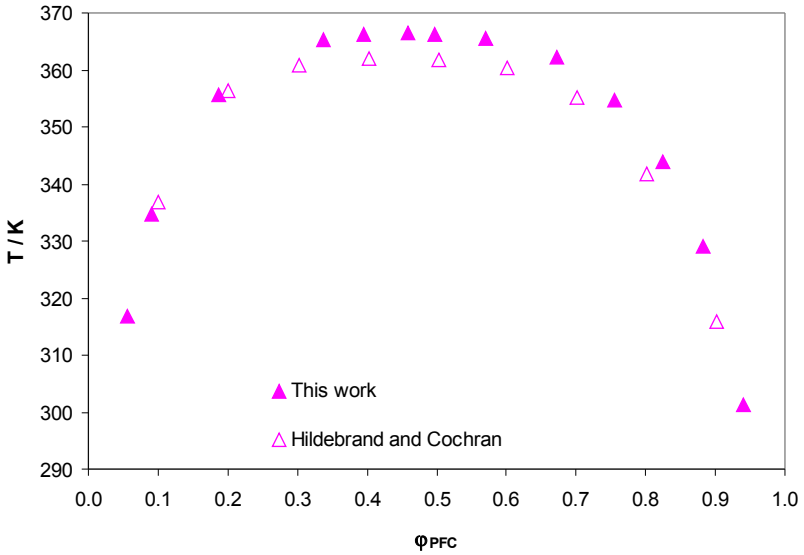

Figure 3.4. Experimental data of perfluoromethylcyclohexane + toluene system in terms of volume fraction. The non-filled symbol represent Hildebrand and Cochran data.[13]

3.2 Determination of the Upper Critical Solution Temperature

The LLE data measured for all the systems is presented in Figure 3.5 in terms of reduced coordinates. Although this highlights the similarity of the studied systems, it will be shown in the next section marked differences between them.

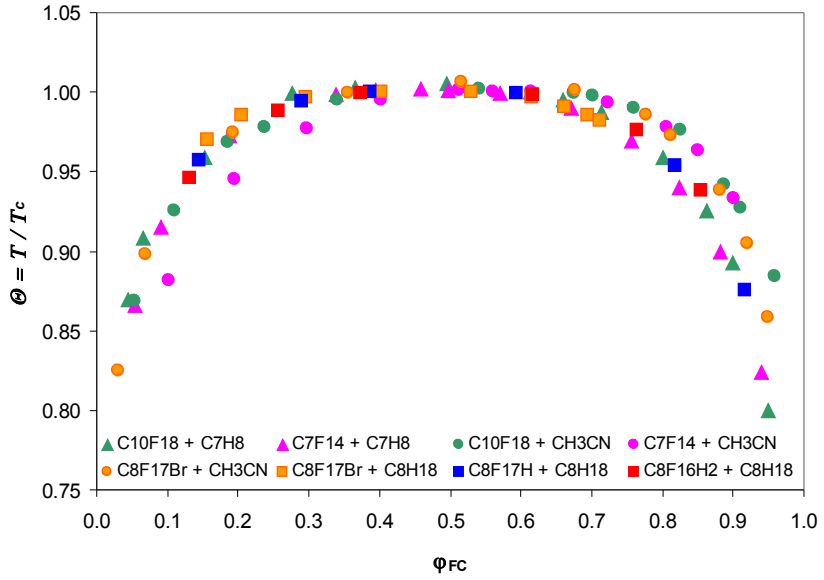

Figure 3.5. Liquid-liquid coexistence curves plotted in reduced coordinates for all the studied systems.

The renormalization group (RG) theory, can be used to represent liquid-liquid equilibrium of mixtures that have an exact symmetry at the critical point with respect to a proper order parameter (p).[46] Mole fraction, volume fraction, weight fraction and mass density are some possible order parameters. As it was observed before in Figures 3.1-3.4 and confirmed in Figure 3.5, experimental data of these studied systems indicate that the volume fraction representation is more symmetric than other representations, as for example mole fraction, and thus volume fraction was chosen as the order parameter.

The critical exponent β defines the shape of the coexisting curve as $\tau=(T_c-T)/T_c$ nears zero:

$$\Delta p = B\tau^{\beta} \tag{2}$$

where Δp is the difference between the order parameters of coexisting phases.

Other terms were added to describe the diameter of coexistence curve over a wide range of temperatures. The relationship that better correlates the experimental data measured in this work is written in the following form:

$$\varphi-\varphi_c = f\alpha\left(\frac{T_c-T}{T_c}\right)^{\beta} \tag{3}$$

where $f=1$ for $\varphi > \varphi_c$ and $f=-1$ for $\varphi < \varphi_c$.

The correlation derived from RG theory is represented together with respective experimental data in Figures 3.6 and 3.7. In Table 3.1 the values of parameters (α, β) and critical constants (φ_c, T_c) obtained from Equation (3) for each system studied are reported. The corresponding critical mole fractions are also presented in Table 3.1.

Table 3.1. Parameters used to correlate data from RG theory and critical constants for studied systems.

System	α	β	φ_c	x_c	T_c / K
$C_{10}F_{18}$ + C_7H_8	0.6752	0.2169	0.4756	0.2864	366.53
C_7F_{14} + C_7H_8	0.7246	0.2600	0.4797	0.3328	365.78
$C_{10}F_{18}$ + CH_3CN	0.7535	0.2437	0.5140	0.1883	443.33
C_7F_{14} + CH_3CN	0.8688	0.3195	0.5417	0.2406	432.70
$C_8F_{17}Br$ + CH_3CN	0.6665	0.1986	0.4994	0.1673	406.87
$C_8F_{17}Br$ + C_8H_{18}	0.7542	0.2673	0.4521	0.3400	279.69
$C_8F_{17}H$ + C_8H_{18}	0.7540	0.2600	0.4785	0.3835	329.29
$C_8F_{16}H_2$ + C_8H_{18}	0.8305	0.2911	0.4853	0.4004	327.85

3.3 LLE with interest in FBS

Six different FBS were investigated: three different FCs were studied with two organic solvents. Two cyclic PFCs were selected (perfluorodecalin and PFMCH) and a substituted linear FC (1Br-perfluoro-*n*-octane). The organic compounds used were toluene and acetonitrile.

In Table 3.2 LLE data for both studied systems that contain perfluorodecalin are presented and in Table 3.3 the values for PFMCH + acetonitrile and perfluoro-*n*-octylbromide + acetonitrile systems are listed. In both Tables, the system composition is presented in mole, weight and volume fractions, together with the cloud point temperature and respective standard deviation.

Table 3.2. Experimental LLE data for systems with perfluorodecalin.

$C_{10}F_{18}$ + C_7H_8				$C_{10}F_{18}$ + CH_3CN			
x_{PFC}	w_{PFC}	φ_{PFC}	(T ± σ[a]) / K	x_{PFC}	w_{PFC}	φ_{PFC}	(T ± σ[a]) / K
0.0201	0.0933	0.0443	318.77 ± 0.07	0.0126	0.1258	0.0551	384.97 ± 0.07
0.0305	0.1364	0.0664	332.83 ± 0.11	0.0264	0.2341	0.1102	410.18 ± 0.02
0.0741	0.2864	0.1532	351.54 ± 0.11	0.0474	0.3589	0.1849	429.38 ± 0.19
0.1447	0.4590	0.2766	366.28 ± 0.08	0.0640	0.4349	0.2377	433.65 ± 0.11
0.2031	0.5610	0.3655	367.46 ± 0.11	0.1018	0.5607	0.3408	441.15 ± 0.16
0.3026	0.6852	0.4951	368.52 ± 0.04	0.2060	0.7450	0.5420	444.07 ± 0.03
0.4128	0.7790	0.6137	366.60 ± 0.02	0.3124	0.8365	0.6745	443.14 ± 0.04
0.4611	0.8110	0.6591	364.76 ± 0.06	0.3409	0.8534	0.7023	442.17 ± 0.14
0.5237	0.8465	0.7131	361.85 ± 0.07	0.4107	0.8869	0.7606	438.97 ± 0.16
0.6397	0.8990	0.8005	351.47 ± 0.03	0.5087	0.9210	0.8252	432.90 ± 0.21
0.7345	0.9328	0.8621	339.12 ± 0.10	0.6363	0.9517	0.8886	417.35 ± 0.06
0.7972	0.9517	0.8988	327.35 ± 0.19	0.6915	0.9619	0.9109	410.88 ± 0.08
0.8929	0.9766	0.9496	293.09 ± 0.51	0.8414	0.9835	0.9603	392.06 ± 0.04

[a] Standard deviation

The data for 1Br-perfluoro-*n*-octane + toluene are not presented because the clear identification of the cloud points was not possible. A gradual change in color occurred, probably due to a slow kinetics, but the exact moment of phase

separation could not be precisely detected. In this case, it is clear that a different experimental method, for example, laser light scattering, would be very helpful.[44]

Table 3.3. Experimental LLE data of PFMCH + acetonitrile and perfluoro-*n*-octylbromide + acetonitrile systems.

C_7F_{14} + CH_3CN				$C_8F_{17}Br$ + CH_3CN			
x_{PFC}	w_{PFC}	φ_{PFC}	(T ± σ[a]) / K	x_{PFC}	w_{PFC}	φ_{FC}	(T ± σ[a]) / K
0.0297	0.2067	0.1023	381.59 ± 0.10	0.0062	0.0708	0.0302	365.26 ± 0.10
0.0609	0.3563	0.1949	409.13 ± 0.03	0.0148	0.1543	0.0693	349.31 ± 0.03
0.1020	0.4921	0.2977	422.62 ± 0.04	0.0460	0.3696	0.1932	335.50 ± 0.02
0.1525	0.6055	0.4017	430.59 ± 0.08	0.1000	0.5746	0.3556	395.63 ± 0.06
0.2200	0.7063	0.5126	432.96 ± 0.03	0.1768	0.7231	0.5161	396.50 ± 0.02
0.2558	0.7456	0.5618	432.85 ± 0.06	0.2970	0.8370	0.6772	400.87 ± 0.03
0.2994	0.7847	0.6145	432.67 ± 0.05	0.4126	0.8952	0.7771	406.65 ± 0.06
0.4118	0.8566	0.7231	429.90 ± 0.04	0.4669	0.9141	0.8130	408.02 ± 0.08
0.5273	0.9049	0.8062	423.19 ± 0.04	0.6032	0.9487	0.8830	407.13 ± 0.09
0.6061	0.9292	0.8516	416.83 ± 0.04	0.7004	0.9660	0.9207	381.78 ± 0.05
0.7097	0.9542	0.9012	403.80 ± 0.15	0.7948	0.9792	0.9506	368.00 ± 0.03

[a] Standard deviation

Analyzing Figure 3.6, systems containing acetonitrile have a higher T_c than those containing toluene, independently of the FC considered. Interesting to note is the fact that the systems containing toluene present very similar LLE diagrams, with T_c that are very close to each other, while when acetonitrile was used a clear separation of the phase diagrams was obtained.

The mutual solubilities can be explained by the simple rule “like dissolves like” using polarity of the involved compounds: polarity will limit the attractive interactions (i.e. dispersive forces) between molecules. As it can be seen in Table 1.2, both organic solvents used are polar compounds and acetonitrile has a dipole moment (13.08×10^{-30} C.m) one order of magnitude larger than toluene (1.25×10^{-30} C.m). Thus, acetonitrile, the most polar compound, is the one that has the highest solubilities with perfluoro-*n*-octylbromide, that is the less apolar FC studied and

has the lowest solubilities with perfluorodecalin, an apolar perfluorocompound.

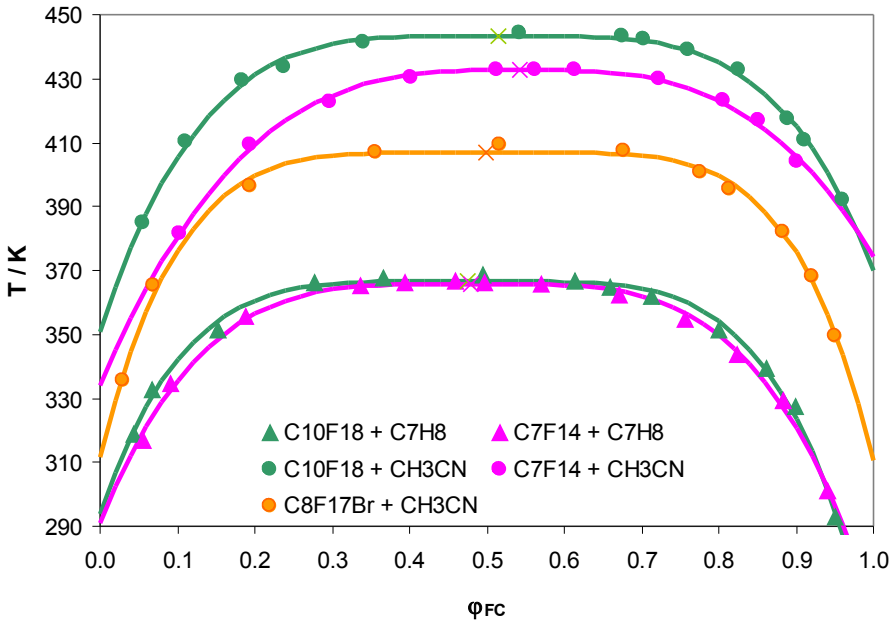

Figure 3.6. Experimental data in terms of volume fraction of studied FC + toluene and FC + acetonitrile systems. (X) Represents the UCST for each mixture. The lines represent the correlated data calculated from RG theory.

3.4 Systems with *n*-octane

The LLE behavior of three different substituted perfluoro-*n*-octanes + *n*-octane systems were also studied within this work. The aim of this particular study was to explore the effect of the introduction of different substitutes at the end of perfluoro-*n*-octane chain in the phase equilibria comparing the results with the LLE data for the completed fluorinated perfluoro-*n*-octane.[45] The selected substituted compounds contain one bromide atom at the end of the chain, one hydrogen atom at the end of the chain and two hydrogens atoms in opposite extremes of chain. Another systems that could be of value in the present context are 1Cl-perfluoro-*n*-octane + *n*-octane, but the fluorinated compound is not commercially available, and 1I-perfluoro-*n*-octane + *n*-octane but the FC is light sensible, so it could not be used in the present setup.

In Figure 3.7 the measured experimental equilibrium results are presented and the data are listed in Tables 3.4 and 3.5. The results obtained by Melo et al.[45] for the system perfluoro-*n*-octane + *n*-octane are also represented.

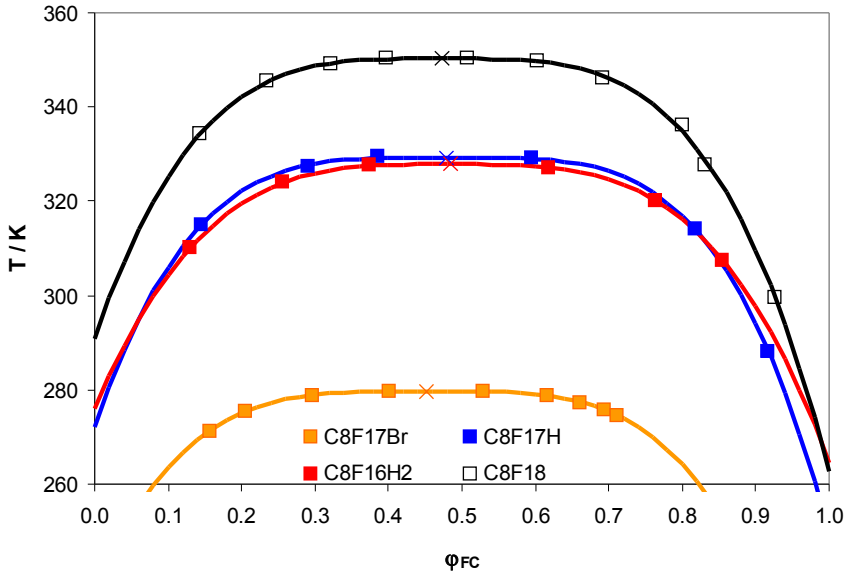

Figure 3.7. Experimental data in terms of volume fraction of substituted perfluoro-*n*-octane + *n*-octane. (X) Represents the UCST for each mixture. The non-filled symbol represent Melo et al. data[45]. The lines represent the correlated data calculated from RG theory.

It is very interesting to notice that the introduction of one or two substitute at the end of the chain promotes the mutual solubility between the fluorocarbon under study and the *n*-octane. The studied compounds present the following order of solubilities in *n*-octane:

$$C_8F_{18} < C_8F_{17}H \approx C_8F_{16}H_2 < C_8F_{17}Br$$

As it was mentioned before, fluorine extreme electronegativity and relatively low polarizability is responsible for the strong strength of the C-F bond (116 kcal.mol^{-1})[16], which is the strongest bond formed with carbon, and with weak intermolecular interactions. The substitution of one fluorine atom by an hydrogen or bromide atom will originate weaker intramolecular bonds, where C-H bond (99 kcal.mol^{-1})[16] and the C-Br bond (68 kcal.mol^{-1})[16], and higher intermolecular interactions. These facts can explain the solubility order obtained in the experimental equilibria data.

Although the introduction of one H atom has a marked effect on the phase equilibria, the introduction of the second H in the opposite end of the chain has hardly no effect. This indicates that there is a geometrical factor, an entropic factor, governing the phase equilibria, since the second H in the FC does not contribute, does not interact, with the *n*-octane (Table 3.4).

Table 3.4. Experimental data of 1H-perfluoro-*n*-octane + *n*-octane and 1H,8H-perfluoro-*n*-octane + *n*-octane systems.

$C_8F_{17}H + C_8H_{18}$				**$C_8F_{16}H_2 + C_8H_{18}$**			
x_{PFC}	w_{PFC}	φ_{FC}	(T ± σ[a]) / K	x_{PFC}	w_{PFC}	φ_{FC}	(T ± σ[a]) / K
0.1032	0.2974	0.1452	315.06 ± 0.05	0.0962	0.2726	0.1307	310.20 ± 0.02
0.2168	0.5044	0.2899	327.45 ± 0.07	0.1964	0.4625	0.2566	324.04 ± 0.08
0.2988	0.6104	0.3860	329.34 ± 0.01	0.2970	0.5979	0.3737	327.54 ± 0.05
0.4986	0.7853	0.5946	329.06 ± 0.04	0.5332	0.8008	0.6173	327.19 ± 0.04
0.7532	0.9182	0.8183	313.97 ± 0.02	0.6960	0.8896	0.7638	320.12 ± 0.03
0.8826	0.9651	0.9173	288.21 ± 0.18	0.8073	0.9365	0.8554	307.49 ± 0.14

[a] Standard deviation

For the perfluoro-*n*-octylbromide + *n*-octane system, it was not possible to clear detect the LLE region for volume fraction of FC lower than 0.15 and higher than 0.72. As in the case of 1Br-perfluoro-*n*-octane + toluene system, a slow change in color was noticed, but no cloud points were obtained. On the other hand, when the system was submitted to sufficiently low temperatures a SLE (solid-liquid equilibrium) region was found. So, all the ampoules of this system were measured in order to identify the SLE diagram. The results of SLE together with LLE of this particular system are presented in Table 3.5 and illustrated in Figure 3.8.

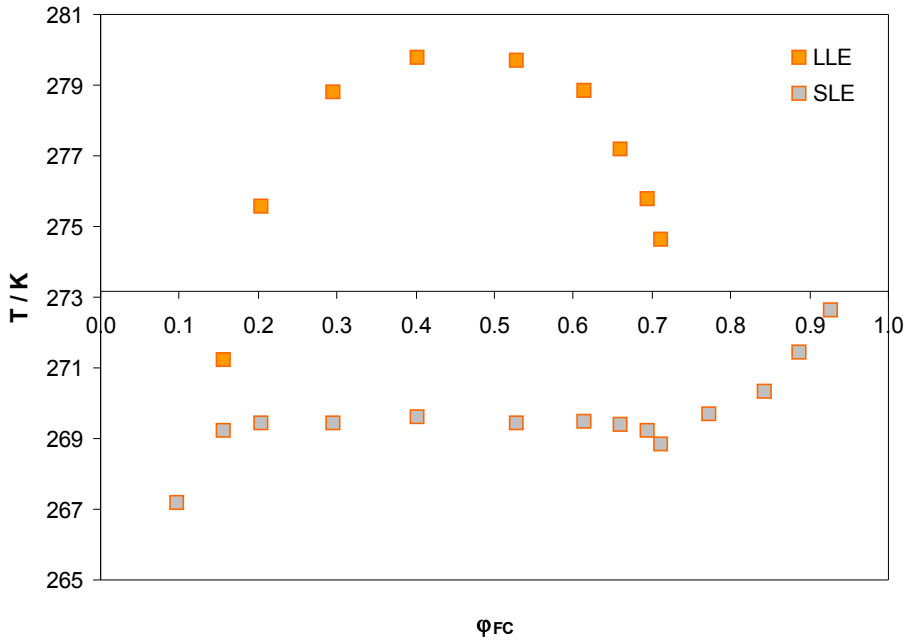

Figure 3.8. Experimental data (LLE and SLE) in terms of volume fraction of 1Br-perfluoro-*n*-octane + *n*-octane binary system.

After these results were obtained, it seamed interesting to study the effect of the presence of two atoms of Br in opposite ends of the FC chain. However, the 1Br,8Br-perfluoro-*n*-octane is solid at room temperature which invalidated the study. This fact lead to the choice of 1Cl,8Cl-perfluoro-*n*-octane + *n*-octane system. One ampoule of this system was prepared and measured, but only SLE

was observed. The mole fraction of the prepared mixture was 0.4112 and the respective cloud point temperature measured was 269.99 K.

Table 3.5. Experimental data (LLE and SLE) of perfluoro-*n*-octylbromide + *n*-octane

$C_8F_{17}Br + C_8H_{18}$ (LLE)				**$C_8F_{17}Br + C_8H_{18}$ (SLE)**			
x_{PFC}	w_{PFC}	φ_{FC}	T ± σ[a] (K)	x_{PFC}	w_{PFC}	φ_{FC}	T ± σ[a] (K)
0.1040	0.3366	0.1568	271.22 ± 0.03	0.0630	0.2270	0.0972	267.18 ± 0.07
0.1384	0.4122	0.2045	275.54 ± 0.03	0.1040	0.3366	0.1568	269.20 ± 0.13
0.2078	0.5340	0.2959	278.78 ± 0.01	0.1384	0.4122	0.2045	269.44 ± 0.10
0.2956	0.6470	0.4019	279.76 ± 0.04	0.2078	0.5340	0.2959	269.42 ± 0.09
0.4126	0.7542	0.5294	279.68 ± 0.05	0.2956	0.6470	0.4019	269.60 ± 0.15
0.4998	0.8136	0.6154	278.81 ± 0.04	0.4126	0.7542	0.5294	269.44 ± 0.15
0.5489	0.8417	0.6609	277.19 ± 0.04	0.4998	0.8136	0.6154	269.47 ± 0.08
0.5861	0.8608	0.6940	275.76 ± 0.05	0.5489	0.8417	0.6609	269.38 ± 0.10
0.6063	0.8706	0.7115	274.61 ± 0.05	0.5861	0.8608	0.6940	269.19 ± 0.09
				0.6063	0.8706	0.7115	268.82 ± 0.09
				0.6797	0.9552	0.7727	269.70 ± 0.06
				0.7711	0.9364	0.8436	270.34 ± 0.06
				0.8299	0.9552	0.8865	271.42 ± 0.04
				0.8876	0.9718	0.9267	272.62 ± 0.07

[a] Standard deviation

4 MODELING

Experimental measurements are time-consuming and often expensive, thus promoting the use of correlations and/or models, such as soft-SAFT EoS, allowing to predict the behavior of a wide number of systems that by experimental determination would be inviable.

To overcome the inability of applying EoS in the absence of data and be able to reduce the amount of experimental work needed, it is necessary to fine tune predictive thermodynamic models, such as COSMO-RS that is a model based on molecular quantum chemical calculations, in such a way that reliable information can be obtained.

In this chapter both approaches will be applied to experimental data and the results will be discussed.

4.1 soft-SAFT

The van der Waals equation and its variations, such as most of the conventional engineering equations of state (Peng-Robinson, Soave-Redlich-Kwong, modified Benedict-Webb-Rubin), are based on the concept of considering a hard-sphere reference term to represent the repulsive interactions and a mean-field term to account for the dispersion and any other long-range forces.

Recently, the development of molecular based equations of state (EoS) represent a important break through in the accurate understanding and prediction of the behavior of complex fluids in extreme conditions, for which other classical methods fail. Due to its robustness, versatility and elegance, the **S**tatistical **A**ssociating **F**luid **T**heory (SAFT), and its different versions, is becoming increasingly popular in academia and industry. All SAFT-type equations are based on Wertheim's first-order thermodynamic perturbation theory (TPT1) for the chain and association term,[47-49] but differ on the intermolecular potential chosen to describe the reference fluid: in the original SAFT approach, the reference fluid is the hard-sphere model, in the PC-SAFT a chain of hard spheres is considered, in the SAFT-VR a square well potential with variable range was used and in the soft-SAFT approach, used in this work, the reference fluid is described by the Lennard-

Jones intermolecular potential. Despite the direct connection of the EoS parameters to intermolecular parameters that all these SAFT models present, the great novelty about this family of equations is to account explicitly for specific interactions, such as hydrogen bonding. Thus, this theory enables a more correct description and understanding of complex fluid behaviors and can predict more accurately the behavior of a wide variety of industrial relevant mixtures.

The general expression for SAFT is usually written in terms of the residual molar Helmholtz energy (A^{res}), defined as the molar Helmholtz energy of the fluid relative to that of an ideal gas, at the same temperature and density. The general expression of the SAFT equation can be written as a sum of four terms:

$$A^{res} = A^{total} - A^{ideal} = A^{ref} + A^{chain} + A^{assoc} + A^{polar} \quad (4)$$

where A^{ref} refers to the contribution due to intermolecular interactions of the reference system, A^{chain} evaluates the free energy due to the formation of a chain from units of the reference system, A^{assoc} takes into account the contribution due to site-site association and A^{polar} is the contribution due to the presence of specific interactions, such as polar interactions due to the presence of dipoles or quadrupoles. For molecules that do not associate, the association term is null. A more detailed description of each term can be found in Appendix C.

The soft-SAFT was presented in 1997 by Blas and Vega and it has been successfully used in several applications.[50-54] This particular modification of the original equation, also based on Wertheim's TPT1, uses the Lennard-Jones (LJ) potential for the reference fluid, which accounts in a single term for dispersive and repulsive forces, while the original equation uses a perturbation scheme based on a hard-sphere fluid + dispersion contribution. Thus, the reference fluid used in soft-SAFT EoS simplifies the overall perturbation approach, since the repulsive and dispersive contributions are taken into account simultaneously.

Within the SAFT context three parameters are considered to describe a molecule: the number of segments (*m*), the diameter of each segment (σ) and its interaction energy (ε). Two additional parameters are used for associating

molecules: one represents the volume occupied by the association site bonded to another associating molecule (k_{HB}), and the other is related to the energetic strength of the association (ε_{HB}). These parameters are usually obtained by fitting the equation to density and vapor pressure data of the pure compounds. Whenever necessary, the polar interactions are accounted for by introducing extra parameters. For example, the magnitude of the quadrupole is described by an additional parameter, the quadrupole moment (Q), and it is modeled as being effectively present in a fraction of the segments of the molecule (x_p). Two binary interaction parameters, from generalized Lorentz-Berthelot combination rules, can be used to provide an accurate description of mixture data: η and ξ, accounting for differences in size and energy of the segments on the different compounds present in the mixture. When no binary interaction parameter is used, the value of these parameters is the unity and the results obtained for the mixture behavior are predictive.

4.1.1 Results and discussion

To adequately describe the phase behavior of a mixture with the soft-SAFT EoS, the molecular parameters for the pure compounds used have to be known. These parameters are available in the literature for all the studied compounds, except for the acetonitrile and are listed in Table 4.1, along with their respective sources, for sake of clearness. Only for acetonitrile, three molecular parameters (m, σ and ε) were adjusted in the present work, using vapor pressure and liquid density data.[55] The results obtained from these fits are presented in Figure 4.1 and Figure 4.2 and they indicate the good description of these properties by the soft-SAFT Eos, with an AAD less than 5.74 % for vapor pressure and 1.68 % for the liquid density. It should be mentioned that acetonitrile is a polar molecule, with a large dipole moment (see Table 1.2), which was not accounted for in an explicitly way in our model. Note, however, that the fit of 4 instead of 3 parameters for acetonitrile would not be noticed in terms of the pure compound properties, since

the other 3 parameters are being adjusted simultaneously. The same kind of results occurred when CO_2 parameters were fitted with and without the quadrupole moment.[56]

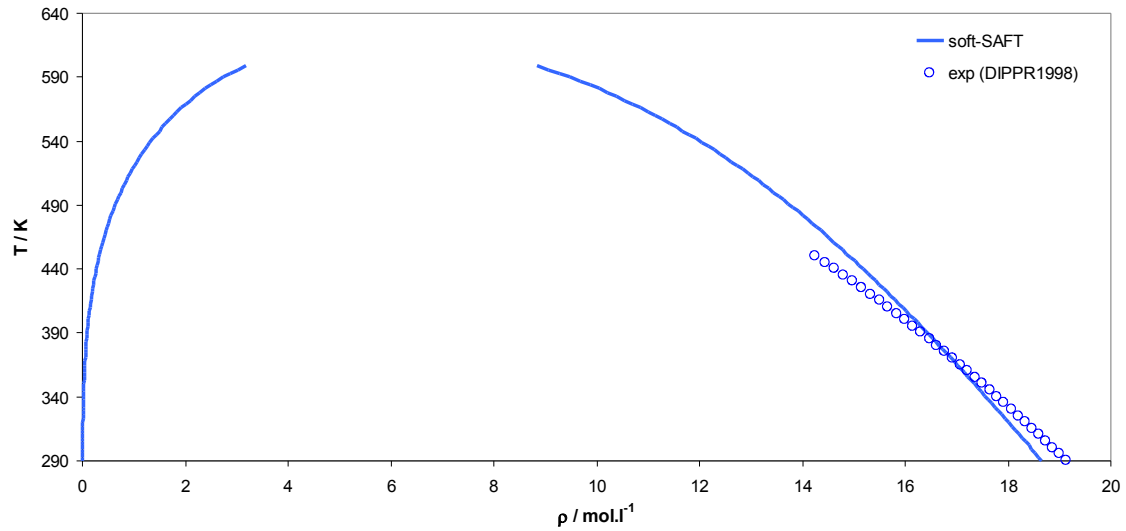

Figure 4.1. Densities of pure acetonitrile. Symbols are experimental data from the DIPPR data base (1998)[55], line correspond to the soft-SAFT model with optimized parameters.

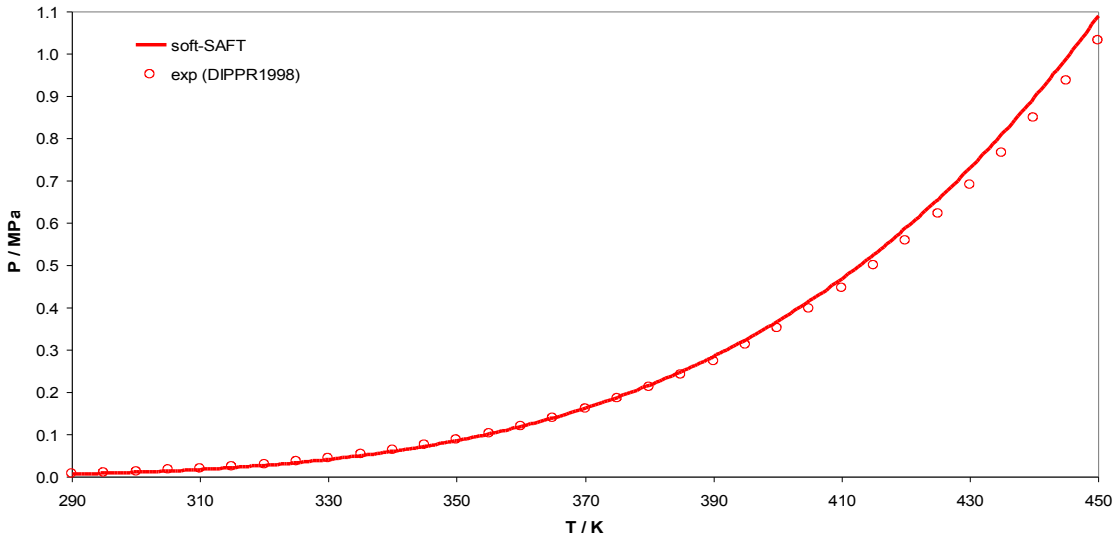

Figure 4.2. Vapor pressures of pure acetonitrile. Symbols are experimental data from the DIPPR data base (1998)[55], line correspond to the soft-SAFT model with optimized parameters.

Table 4.1. Parameters used in soft-SAFT EoS for the compounds present in studied systems.

Compound	*m*	σ / Å	(ε/k_B) / K	Q / (10^{-40} C m^2)	reference
$C_{10}F_{18}$	2.696	4.999	310.1	-	[17]
C_7F_{14}	3.463	4.15	228.6	-	[56]
$C_8F_{17}Br$	3.522	4.652	268.9	-	[17]
$C_8F_{17}H$	3.522	4.492	253.6	-	[17]
$C_8F_{16}H_2$	3.522	4.456	267.8	-	[57]
C_8F_{18}	3.522	4.521	245.1	-	[51]
CH_3CN	2.435	3.142	309.9	-	this work, [55]
C_7H_8	2.692	3.925	296.5	-5.0	[21]
C_8H_{18}	3.522	3.970	264.4	-	[51]

The results obtained when soft-SAFT is used to correlate the behavior of FCs (perfluorodecalin, PFMCH or perfluoro-*n*-octylbromide) + acetonitrile systems are presented in Figure 4.3. As it can be seen, these systems are not well describe by the model proposed for the mixture. Binary parameters, listed in Table 4.2, were adjusted to provide a more accurate description of these mixtures. The $C_8F_{17}Br$ + CH_3CN system has only one binary parameter adjusted, because it was not possible to obtain better results adjusting both.

Although the largest deviations were obtained in the FCs rich phase, the parameters used for these compounds were already successfully used in other systems and they always presented the correct behavior. This indicates that probably the model proposed for acetonitrile, without taking into account explicitly its large dipole moment, is not the most accurate. Thus, a new improved description of acetonitrile is in need, where the dipole moment is explicitly included. This can be achieved in two ways: by using the polar term or as a specific interaction, described by the association term. The latter was used before in similar cases, like for H_2O and HCl, and the results obtained were quite satisfactory.[58]

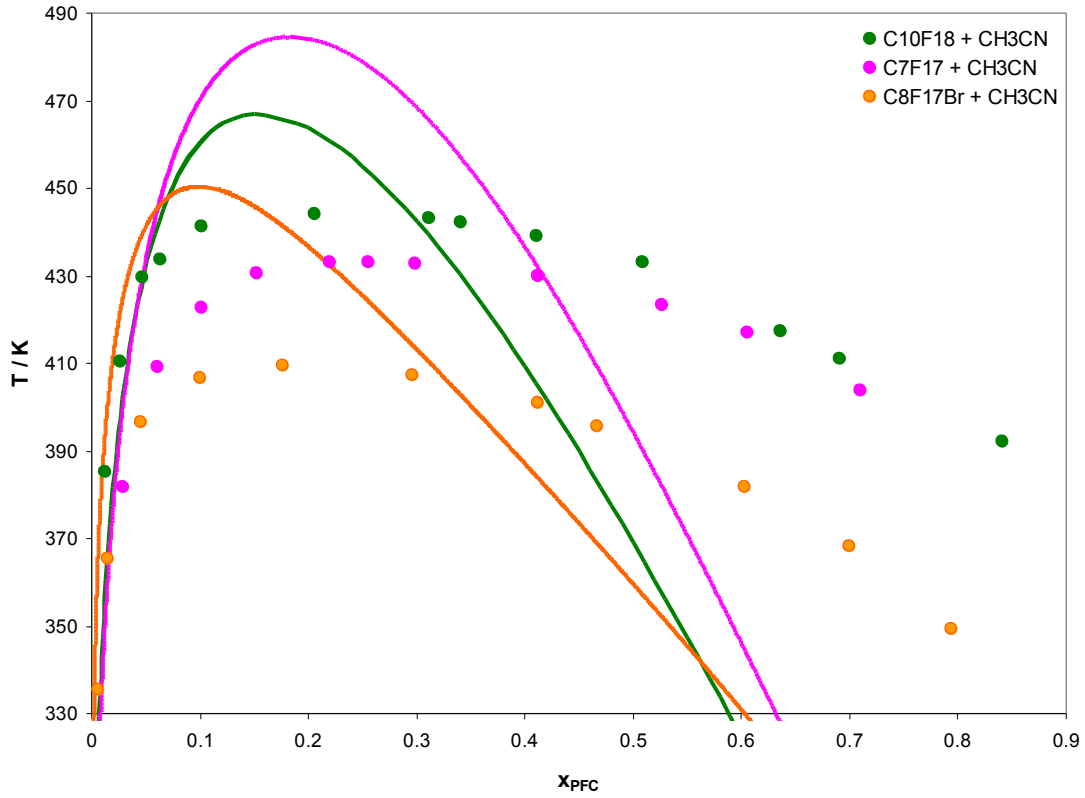

Figure 4.3. Soft-SAFT EoS correlation and liquid-liquid data of fluorocarbons + acetonitrile mixtures, in terms of mole fraction.

Table 4.2. Optimized binary parameters used in soft-SAFT EoS for the studied systems.

Compound	η_{ij}	ξ_{ij}
$C_{10}F_{18}$ + C_7H_8	1.050	0.8746
C_7F_{14} + C_7H_8	1.000	0.8946
$C_{10}F_{18}$ + CH_3CN	0.918	0.8916
C_7F_{14} + CH_3CN	0.918	0.8916
$C_8F_{17}Br$+ CH_3CN	1.000	0.9146
C_8F_{18} + C_8H_{18} [45]	1.000	0.9146
$C_8F_{17}Br$ + C_8H_{18}	1.000	0.9360
$C_8F_{17}H$ + C_8H_{18}	1.000	0.9207
$C_8F_{16}H_2$ + C_8H_{18}	1.000	0.9189

The results obtained with soft-SAFT EoS for cyclic PFCs' mixtures with toluene are in good agreement with the experimental data (Figure 4.4) although the critical region is overestimated. Note that in the case of $C_{10}F_{18}$ + C_7H_8 two binary parameters were needed to obtain the present correlation, while in the case of C_7F_{14} + C_7H_8 only one parameter is needed. As any other analytical EoS, soft-SAFT is unable to correctly describe the scaling of thermodynamic properties as the critical point is approached giving systematically higher predictions near this point. The mean-field equations of state provide a reasonable description of fluid equilibrium properties far away from the critical point. However, near the critical point, due to density and/or concentration fluctuations, classical analytical equations fail. Attempts to deal with this problem include the use of a cross-over approach, which has not been so far implemented for the description of LLE with soft-SAFT.

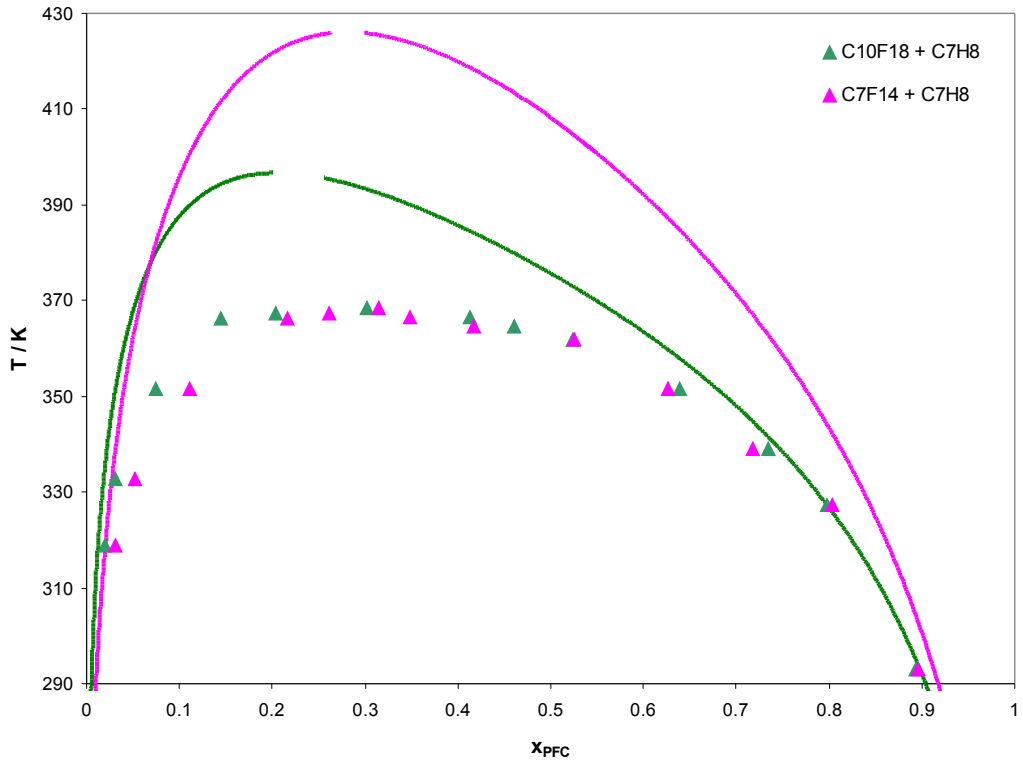

Figure 4.4. Soft-SAFT EoS correlation and liquid-liquid data of perfluorodecalin + toluene and perfluoromethylcyclohexane + toluene mixtures, in terms of mole fraction.

Another point that should be noticed is that soft-SAFT predicts different solubilities for both FCs, being the perfluorodecalin more soluble in toluene than the perfluoromethylcyclohexane, which is not behavior exhibit by the experimental data.

For the substituted fluoro-*n*-octanes mixtures with *n*-octane (Figure 4.5) just the energy interaction parameter was adjusted for each system. A fixed size interaction binary parameter (η = 1) was used because it was verified that the simple Lorentz combination rule provided satisfactory results. The soft-SAFT can qualitatively capture the nature of the studied mixtures, showing the large solubility gap between the 1Br-perfluoro-*n*-octane and the 1H-perfluoro-*n*-octane and 1H,8H-perfluoro-*n*-octane. More exciting is the description the systems containing 1H-perfluoro-*n*-octane and 1H,8H–perfluoro-*n*-octane where no distinction is provided by soft-SAFT for them. This means that the EoS can capture in molecular terms the physical details of these mixtures.

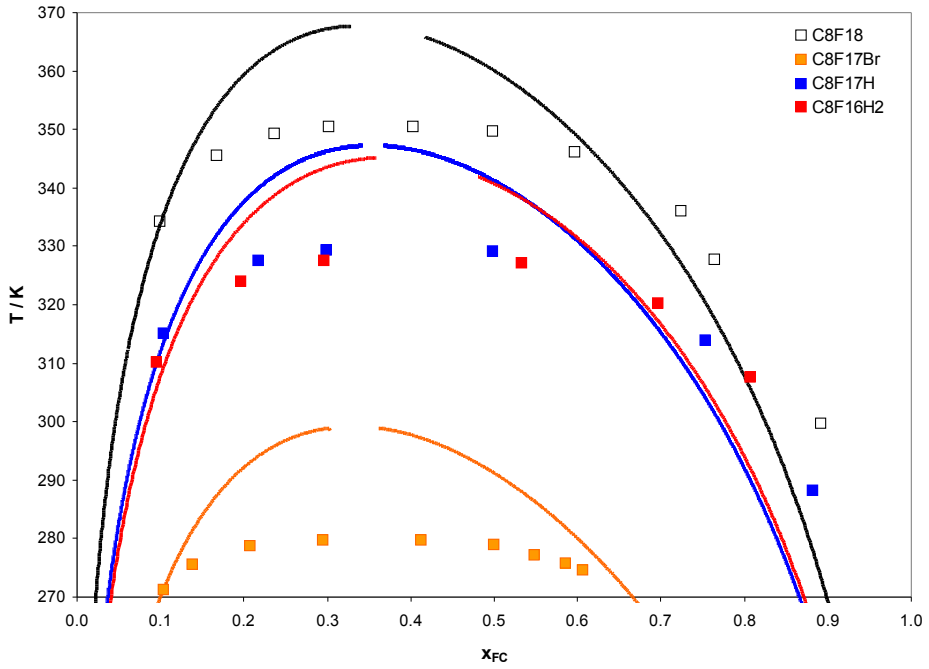

Figure 4.5. Soft-SAFT EoS correlation and liquid-liquid data of substituted perfluoro-*n*-octanes + *n*-octane mixtures, in terms of mole fraction. Comparison with perfluoro-*n*-octane + *n*-octane system.[45]

4.2 COSMO-RS

COnductor-like **S**creening **MO**del for **R**eal **S**olvents (COSMO-RS), proposed by Klamt and co-workers,[59-61] is a novel predictive method for thermodynamic equilibria of fluids and liquid mixtures. It uses a statistical thermodynamics approach based on the results of quantum chemical calculations.

This method has been applied with success, at least qualitatively, in the description of VLE and LLE of ionic liquids and alcohols, hydrocarbons, ketones and water systems. In the present work, COSMO-RS predictive capacity of the phase equilibria behavior of fluorocarbons binary systems is analyzed and the obtained results are compared with the experimental data measured.

In the COSMO calculations, the solute molecules are calculated in a virtual conductor environment, where the solute molecule induces a polarization charge density (σ) on the molecular surface.[62, 63]These charges act back on the solute and generate a more polarized electron density than in vacuum. During the quantum chemical self-consistency algorithm, the solute molecule is, thus, converged to its energetically optimal state in a conductor with respect to electron density. Although time-consuming, one advantage of this procedure is that these calculations have to be performed just once for each molecule of interest.

The (3D) polarization density distribution on the surface of each molecule X_i is converted into a distribution-function, the so called σ-profile, $p^{X_i}(\sigma)$, which gives the relative amount of surface with polarity σ on the surface of the molecule. When a mixture is considered, the σ-profile of the solvent S, $p_S(\sigma)$, can be written as a sum of the $p^{X_i}(\sigma)$ of the components weighted by their mole fraction (x_i) in the mixture.

$$p_S(\sigma)=\sum_{i\in S} x_i p^{X_i}(\sigma) \qquad (5)$$

In statistical thermodynamics calculations is convenient to consider a normalized ensemble and since the integral of $p^{X_i}(\sigma)$ over the entire σ-range is the total surface area A^{X_i} of a compound X_i, the normalized σ-profile, $p'_S(\sigma)$,

of the overall system is defined as follows:

$$p'_S(\sigma) = \frac{p_S(\sigma)}{\sum_{i \in S} x_i A^{X_i}} \quad (6)$$

The most important molecular interaction energy modes, i.e. electrostatics (E_{misfit}) and hydrogen bonding (E_{HB}) are described as functions of the polarization charges of two interacting surface segments σ and σ' or $\sigma_{acceptor}$ and σ_{donor}, if the segments are located on a hydrogen bond donor or acceptor atom (Eq. (7) and Eq.(8)). The van der Waals energy (E_{vdW}) is dependent only on the elements of the atoms involved (Eq. (9)).

$$E_{misfit}(\sigma, \sigma') = a_{eff} \frac{\alpha'}{2} (\sigma + \sigma')^2 \quad (7)$$

$$E_{HB} = a_{eff}\, c_{HB}\, min(0; min(0; \sigma_{donor} + \sigma_{HB})\, max(0; \sigma_{acceptor} - \sigma_{HB})) \quad (8)$$

$$E_{vdW} = a_{eff}\, (\tau_{vdW} + \tau'_{vdW}) \quad (9)$$

where α' is the coefficient for electrostatic misfit interactions, a_{eff} is the effective contact area between two surface segments, c_{HB} is the coefficient for hydrogen bond strength, σ_{HB} is the threshold for hydrogen bonding and τ_{vdW} and τ'_{vdW} are element-specific van der Waals' coefficients.

The molecular interactions in the solvent are thus fully described by $p_S(\sigma)$ and the chemical potential differences resulting from these interactions are calculated with an exact statistical thermodynamics algorithm for independently pair-wise interacting surfaces. The COSMO-RS method depends only on a small number of adjustable parameters (predetermined from known properties of individual atoms) and that are not specific for functional groups or type of molecules. Besides, statistical thermodynamics enables the determination of the chemical potential of all components in the mixture and, from these, thermodynamic properties can be derived.

4.2.1 Results and discussion

The aim of the present section is to test the predictive capacity of COSMO-RS for the fluorocarbon binary systems measured within this work by comparing the obtained results with the experimental data (Figures 4.6-4.9).

The quantum chemical COSMO descriptions of the pure FCs and organic solvents were achieved using the BP functional and the triple-ζ valence polarized large basis set (TZVP) and the mutual solubilities calculations were then performed.

The lowest energy isomers conformation for all the compounds studied was used in the COSMO-RS calculations, since previous works proved that the lower energy conformers provide the best qualitative and quantitative predictions in respect to the experimental results.[64, 65]

Analyzing Figure 4.6 it can be seen that COSMO-RS results describe well the LLE tendency behavior of the FBSs studied. This model can predict the solubility differences observed between the different PFCs. Also, a qualitative prediction for the increasing solubility of studied PFCs in toluene, instead of acetonitrile, is obtained. The LLE behavior of perfluoro-*n*-octylbromide + toluene system, that was not possible to measure experimentally using this present methodology, was calculated using COSMO-RS and results are shown in Figure 4.6. It can be observed that the obtained results for this system clearly follow the expected trend, indicating that this method can be used for *a priori* screen the behavior of fluorocarbons with interest in FBSs. Unfortunately, the UCST region of all the studied systems can not be predicted with this model.

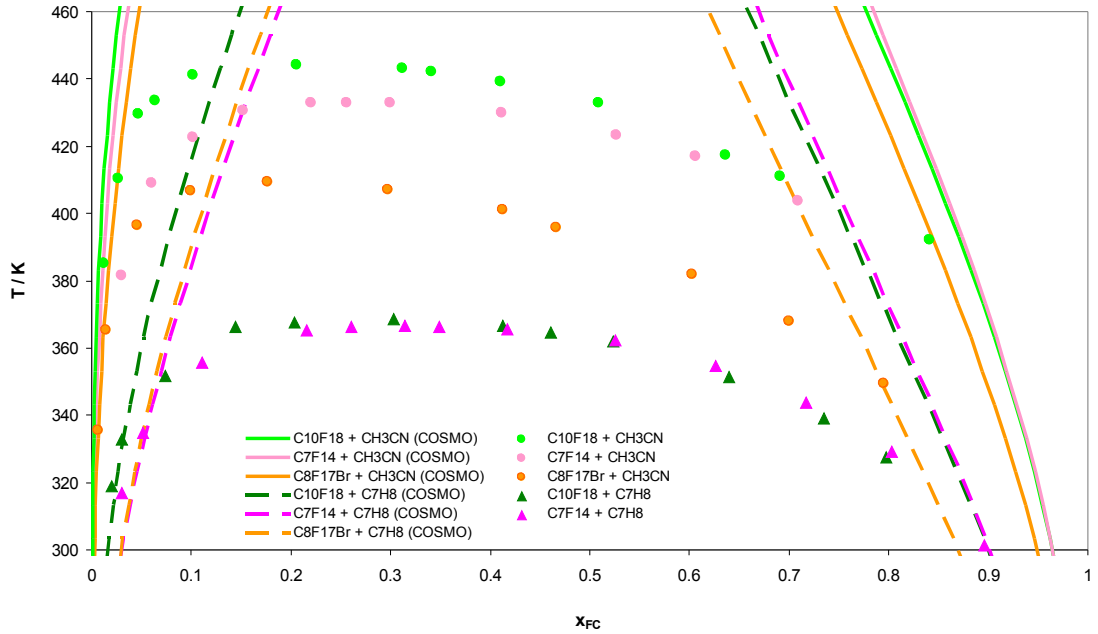

Figure 4.6. COSMO-RS predictions and liquid-liquid data of studied FC + toluene and FC + acetonitrile binary systems, in terms of mole fraction of FC.

The obtained results for the systems with *n*-octane and the substituted FCs do not show the same precision. From the inspection of Figures 4.7-4.9, it can be concluded that the increase of the lipophilic character obtained by the introduction of the bromide FC was neglected, since it predicts similar solubilities for the perfluoro-*n*-octane and for the 1-Br-perfluoro-*n*-octane with *n*-octane. Also, although the introduction of one hydrogen in the perfluoro-*n*-octane solubilities is correctly predicted with respect to the *n*-octane, the introduction of the second hydrogen atom in the opposite extreme end of the chain is regarded as enhancement of the mutual solubility, which is not the case.

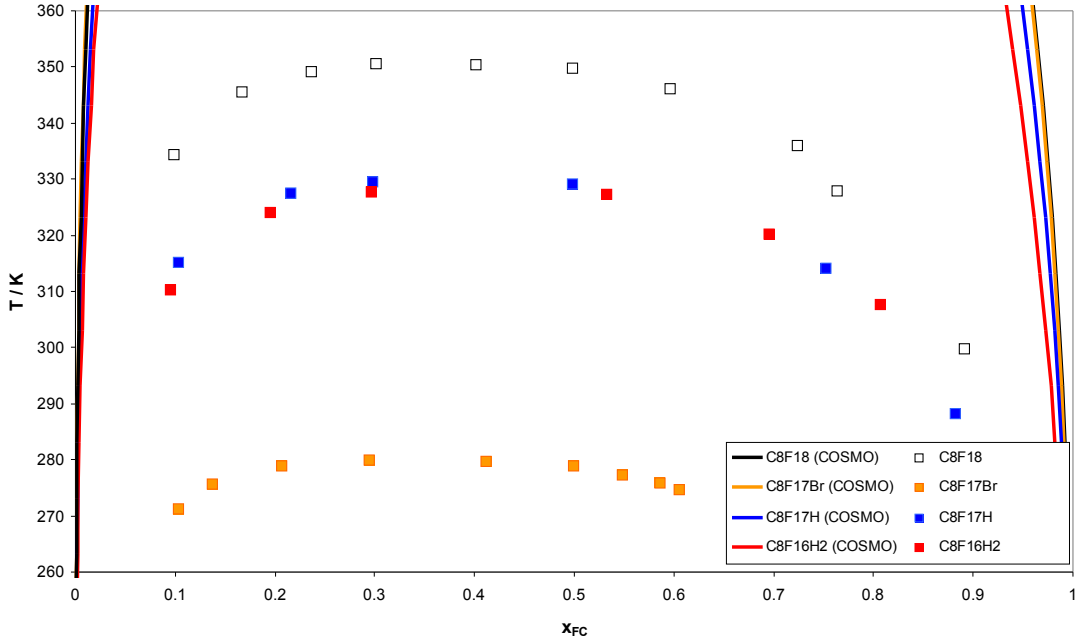

Figure 4.7. COSMO-RS predictions and liquid-liquid data of fluoro-*n*-octane + *n*-octane systems, in terms of mole fraction.

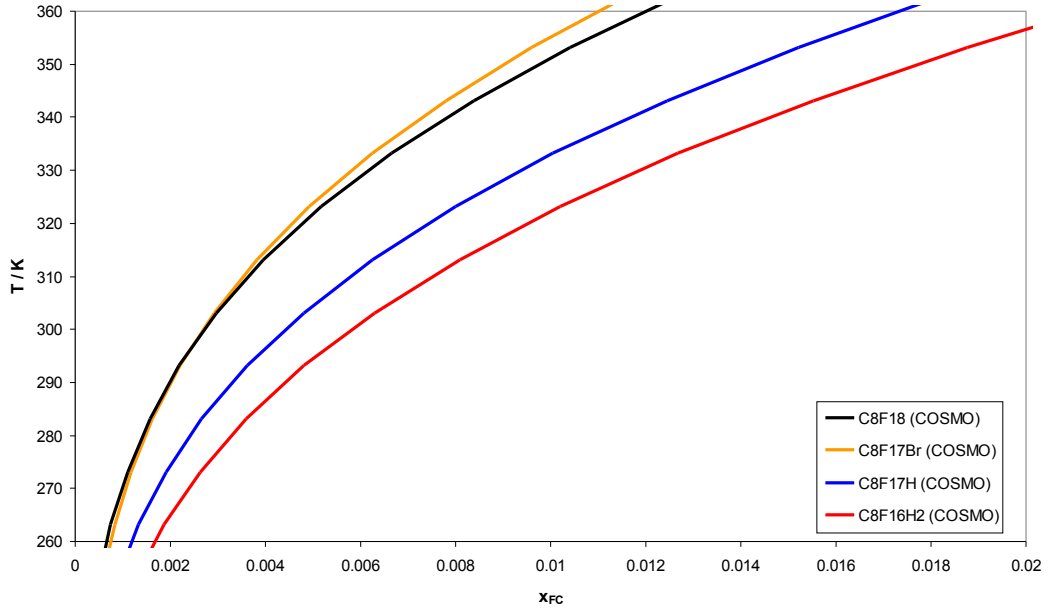

Figure 4.8. COSMO-RS predictions for LLE of *n*-octane rich side.

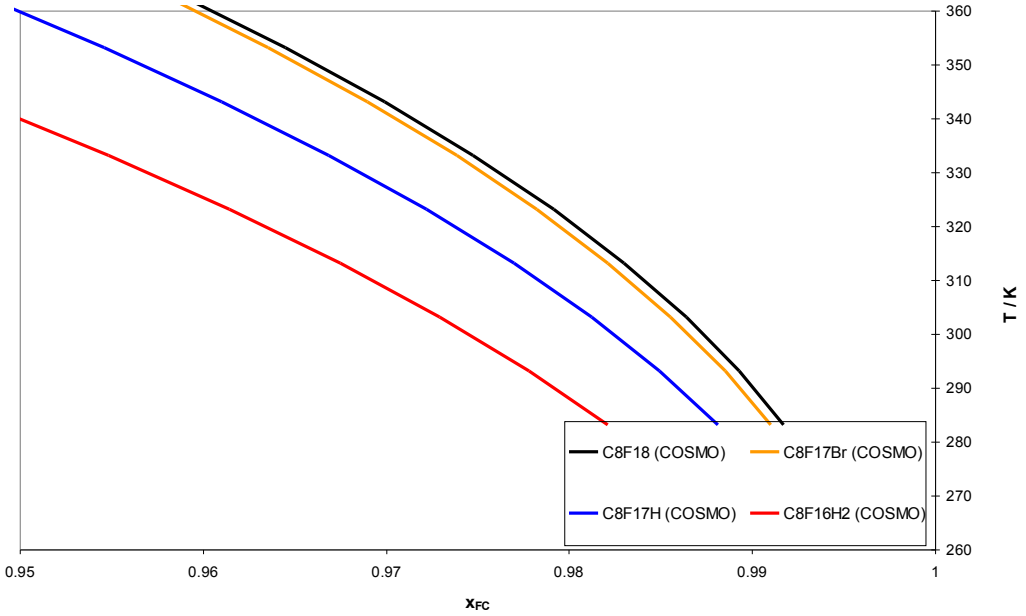

Figure 4.9. COSMO-RS predictions for LLE of fluorinated rich side.

5 Conclusions

5.1 Final Conclusions

Undoubtedly, highly fluorous compounds present a very different behavior when compared with the corresponding hydrocarbons. The original experimental data presented in this dissertation were measured by turbidimetry using the dynamic visual detection method and can help to better characterize the perfluorocarbons and their mixtures. This work contributed also to the enlargement of the database of LLE of highly fluorinated systems, whenever was possible, the systems studied were compared with other systems presented in open literature.

The experimental data were presented in two different perspectives: systems with interesting in FBS and the effect of the introduction of substitutes in fluoro-*n*-octane + *n*-octane systems. In almost every system, the LLE behavior could be correlated to physical properties (such as polarity and molar volume) of the compounds under study.

An effort was made to predict and correlate the LLE these systems using two different approaches:

- Soft-SAFT EoS: The correlation for the cyclic PFCs + toluene systems were quite good, although the critical region were overestimated. On the other hand, systems with PFCs + acetonitrile were not well described with the proposed molecular parameters for the acetonitrile. Finally, the substituted fluoro-*n*-octanes + *n*-octane systems were correlated with soft-SAFT adjusting just the energy interaction parameter for each system, and a fixed size interaction binary parameter equal to unity was used. The soft-SAFT EoS could qualitatively capture the nature of these studied mixture, detecting in molecular terms their physical details.
- COSMO-RS: The results obtained showed to that it is a good tool to predict FBS behavior, but failed on the prediction of the substituted fluoro-*n*-octanes + *n*-octane systems. Furthermore, this model could only give a qualitative behavior, overestimating the mutual solubilities of all studied systems especially close to the critical point.

5.2 Future Work

Despite the great number of studied systems in this dissertation, due to the limited time for the experimental execution, a lot more could be done to complete the present work. The future developments on the field of thermophysical properties of perfluorocarbons should include:

- The construction of an equipment automated for the detection of cloud points using, for example, laser light scattering. It could help in the detection of the phase change of systems with a slow kinetics, like the 1Br-perfluoro-*n*-octane + toluene.
- New soft-SAFT molecular parameters for the acetonitrile, including dipole moment explicitly should be adjusted. The LLE calculations for the respective systems should be re-evaluated.
- In order to understand at the molecular level the interplay between the interaction energies and volume effects in fluoro-*n*-octanes + *n*-octane systems *ab initio* calculations should be performed .
- The measurement of LLE of FC with different substitutes in different positions of the fluorochain, for example, increasing the number of hydrogen atoms in just one extreme of the chain, could further contribute to the study of the behavior LLE of fluorocarbons.

6 REFERENCES

[1] Organizing Committee for the Workshop on Materials and Manufacturing, Committee on Challenges for the Chemical Sciences in the 21st Century, National Research Council; Materials Science and Technology: Challenges for the Chemical Sciences in the 21st Century, The National Academies Press, Washington, D.C. (2003).

[2] W. A. Herrmann, B. Cornils, Organometallic Homogeneous Catalysis - Quo vadis?, *Angewandte Chemie International Edition in English* 36 (1997) 1049.

[3] A. Aghmiz. *Nuevos catalizadores para las reacciones de carbonilación e hidrogenación de alquenos en sistemas homogéneos y bifásicos*. PhD Thesis, Universitat Rovira i Virgili; Departament de Química Física i Inorgànica (2002).

[4] L. P. Barthel-Rosa, J. A. Gladysz, Chemistry in fluorous media: a user's guide to practical considerations in the application of fluorous catalysts and reagents, *Coordination Chemestry Reviews* 192 (1999) 587.

[5] M. Cavazzini, F. Montanari, G. Pozzi, S. Quici, Perfluorocarbon-soluble catalysts and reagents and the application of FBS (fluorous biphase system) to organic synthesis, *Journal of Fluorine Chemistry* 94 (1999) 183.

[6] I. T. Horváth, Fluorous Biphase Chemistry, *Accounts of Chemical Research* 31 (1998) 641.

[7] I. T. Horváth, J. Rábai, Facile Catalyst separation without water - fluorous biphase hydroformylation of olefins, *Science* 266 (1994) 72.

[8] D. Rutherford, J. J. J. Juliette, C. Rocaboy, I. T. Horváth, J. A. Gladysz, Transition metal catalysis in fluorous media: application of a new immobilization principle to rhodium-catalyzed hydrogenation of alkenes, *Catalysis Today* 42 (1998) 381.

[9] D. P. Curran, S. Hadida, Tris(2-(perfluorohexyl)ethyl)tin Hydride: A New Fluorous Reagent for Use in Traditional Organic Synthesis and Liquid Phase Combinatorial Synthesis, *Journal of the American Chemical Society* 118 (1996) 2531.

[10] J. J. J. Juliette, J. A. Gladysz, I. T. Horváth, Transition Metal Catalysis in Fluorous Media: Practical Application of a New Immobilization Principle to Rhodium-Catalyzed Hydroboration, *Angewandte Chemie International Edition in English* 36 (1997) 1610.

[11] J. Vincent, A. Rabion, V. K. Yachandra, R. H. Fish, Fluorous Biphasic Catalysis: Complexation of 1,4,7-[C8F17(CH2)3]3-1,4,7-Triazacyclononane with [M(C8F17(CH2)2CO2)2] (M = Mn, Co) To Provide Perfluoroheptane-Soluble Catalysts for Alkane and Alkene Functionalization in the Presence of t-BuOOH and O2, *Angewandte Chemie-International Edition in English* 36 (1997) 2346.

[12] W. Keim, M. Vogt, P. Wasserscheid, B. Drie[ss]en-Holscher, Perfluorinated polyethers for the immobilisation of homogeneous nickel catalysts, *Journal of Molecular Catalysis A: Chemical* 139 (1999) 171.

[13] J. H. Hildebrand, D. R. F. Cochran, Liquid-Liquid Solubility of Perfluoromethylcyclohexane with Benzene, Carbon Tetrachloride, Chlorobenzene, Chloroform and Toluene, *Journal of the American Chemical Society* 71 (1949) 22.

[14] R. L. Scott, The Solubility of Fluorocarbons, *Journal of the American Chemical Society* 70 (1948) 4090.

[15] I. Klement, H. Lütjens, P. Knochel, Transition Metal Catalyzed Oxidations in Perfluorinated Solvents, *Angewandte Chemie International Edition in English* 36 (1997) 1454.

[16] R. E. Banks, J. C. Tatlow, A guide to modern organofluorine chemistry, *Journal of Fluorine Chemistry* 33 (1986) 227.

[17] A. M. A. Dias, C. M. B. Gonçalves, A. I. Caço, L. M. N. B. F. Santos, M. M. Pineiro, L. F. Vega, J. A. P. Coutinho, I. M. Marrucho, Densities and Vapor Pressures of Highly Fluorinated Compounds, *Journal of Chemical & Engineering Data* 50 (2005) 1328.

[18] Group personal communication.

[19] The NIST Chemistry WebBook at http://webbook.nist.gov/chemistry/

[20] A. M. A. Dias, A. I. Caço, J. A. P. Coutinho, L. M. N. B. F. Santos, M. M. Pineiro, L. F. Vega, M. F. C. Gomes, I. M. Marrucho, Thermodynamic properties of perfluoro-n-octane, *Fluid Phase Equilibria* 225 (2004) 39.

[21] A. M. A. Dias. *Thermodynamic Properties of Blood Substituting Liquid Mixtures*. PhD Thesis, Departamento de Química, Universidade de Aveiro (2005).

[22] A. M. A. Dias, C. M. B. Gonçalves, J. L. Legido, J. A. P. Coutinho, I. M. Marrucho, Solubility of oxygen in substituted perfluorocarbons, *Fluid Phase Equilibria* 238 (2005) 7.

[23] S. Perez-Casas, J. Hernandez-Trujillo, M. Costas, Experimental and Theoretical Study of Aromatic-Aromatic Interactions. Association Enthalpies and Central and Distributed Multipole Electric Moments Analysis, *Journal of Physical Chemistry B* 107 (2003) 4167.

[24] A. Döß, G. Hinze, B. Schiener, J. Hemberger, R. Böhmer, Dielectric relaxation in the fragile viscous liquid state of toluene, *Journal of Chemical Physics* 107 (1997) 1740.

[25] M. G. Freire, L. Gomes, L. M. N. B. F. Santos, I. M. Marrucho, J. A. P. Coutinho, Water Solubility in Linear Fluoroalkanes Used in Blood Substitute Formulations, *Journal of Physical Chemistry B* 110 (2006) 22923.

[26] R. L. Scott, The Anomalous Behavior of Fluorocarbon Solutions, *Journal of Physical Chemistry* 62 (1958) 136.

[27] I. A. McLure, B. Edmonds, Extremes in Surface-tension of Fluorocarbon + Hydrocarbon Mixtures, *Nature* 241 (1973) 71.

[28] J. C. Calado, I. M. McLure, V. Soares, Surface Tension for Octafluorocyclobutane, n-butane and their Mixtures from 233 K to 254 K, and Vapour Pressure, Excess Gibbs Function and Excess Volume for the Mixture at 233 K, *Fluid Phase Equilibria* 29 (1978) 199.

[29] M. P. Krafft, Fluorocarbons and fluorinated amphiphiles in drug delivery and biomedical research, *Advanced Drug Delivery Reviews* 47 (2001) 209.

[30] R. K. Iyer, M. Radisic, C. Cannizzaro, G. Vunjak-Novakovic, Synthetic Oxygen Carriers in Cardiac Tissue Engineering, *Artificial Cells, Blood Substitutes, and Biotechnology* 35 (2007) 135.

[31] A. M. Neubauer, S. D. Caruthers, F. D. Hockett, T. Cyrus, J. D. Robertson, J. S. Allen, T. D. Williams, R. W. Fuhrhop, G. M. Lanza, S. A. Wickline, Fluorine Cardiovascular Magnetic Resonance Angiography In Vivo at 1.5 T with Perfluorocarbon Nanoparticle Contrast Agents, *Journal of Cardiovascular Magnetic Resonance* 9 (2007) 565.

[32] R. P. Mason, S. Ran, P. E. Thorpe, Quantitative assessment of tumor oxygen dynamics: Molecular imaging for prognostic radiology, *Journal of Cellular Biochemistry* 87 (2002) 45.

[33] E. J. Voiglio, L. Zarif, F. C. Gorry, M. Krafft, J. Margonari, X. Martin, J. Riess, J. M. Dubernard, Aerobic Preservation of Organs Using a New Perflubron/Lecithin Emulsion Stabilized by Molecular Dowels, *Journal of Surgical Research* 63 (1996) 439.

[34] S. M. Cohn, Blood Substitutes in Surgery, *Surgery* 127 (2000) 599.

[35] E. K. Rowinsky, Novel Radiation Sensitizers Targeting Tissue Hypoxia, *Oncology (Huntingt)* 13 (1999) 61.

[36] T. R. Porter, F. Xie, A. Kricsfeld, K. Kilzer, Noninvasive Identification of Acute Myocardial-ischemia and Reperfusion with Contrast Ultrasound using Intravenous Perfluoropropane Exposed Sonicated Dextrose Albumin, *Journal of the American College of Cardiology* 26 (1995) 33.

[37] P. Raveendran, S. L. Wallen, Cooperative C-H Center Dot Center Dot Center Dot O Hydrogen Bonding in CO2-Lewis Base Complexes: Implications for Solvation in Supercritical CO2, *Journal of the American Chemical Society* 124 (2002) 12590.

[38] M. G. Freire. *Aeration and Extraction in Multiphase Biological Reactors*. PhD Thesis, Departamento de Química, Universidade de Aveiro (2007).

[39] A. Wasanasathian, C. Peng, Enhancement of Microalgal Growth by Using Perfluorocarbon as Oxygen Carrier, *Artificial Cells, Blood Substitutes & Immobilization Biotechnology* 29 (2001) 47.

[40] A. Goebel, K. Lunkenheimer, Interfacial tension of the water/n-alkane interface, *Langmuir* 13 (1997) 369.

[41] G. Hefter; Liquid-Liquid Solubilities in The Experimental Determination of Solubilities, G. Hefter & R. P. T. Tomkins (Eds.), John Wiley & Sons, Ltd (2003).

[42] J. V. Sengers, J. M. H. L. Sengers, Thermodynamic Behavior of Fluids Near the Critical Point, *Annual Review of Physical Chemistry* 37 (1986) 189.

[43] Corning Labware and Scientific Equipment Catalogue, Corning Ltd. (Ed.), Laboratory Division, U.K (1981).

[44] J. Szydlowski, L. P. Rebelo, W. A. Van Hook, A new apparatus for the detection of phase equilibria in polymer solvent systems by light scattering, *Review of Scientific Instruments* 63 (1992) 1717.

[45] M. J. P. Melo, A. M. A. Dias, M. Blesic, L. P. N. Rebelo, L. F. Vega, J. A. P. Coutinho, I. M. Marrucho, Liquid-liquid equilibrium of (perfluoroalkane + alkane) binary mixtures, *Fluid Phase Equilibria* 242 (2006) 210.

[46] T. Narayanan, A. Kumar, E. S. R. Gopal, S. C. Greer, Liquid-Liquid Critical Phenomena. The Coexistence Curve of n-Heptano-Acetic Anhydride, *Journal of Physical Chemistry* 84 (1980) 2883.

[47] M. S. Wertheim, Fluids with Highly Directional Attractive Forces. I. Statistical Thermodynamics, *Journal of Statistical Physics* 35 (1984) 19.

[48] M. S. Wertheim, Fluids with Highly Directional Attractive Forces. II. Thermodynamic Perturbation Theory and Integral Equations, *Journal of Statistical Physics* 35 (1984) 35.

[49] M. S. Wertheim, Fluids with Highly Directional Attractive Forces. III. Multiple Attraction Sites, *Journal of Statistical Physics* 42 (1986) 459.

[50] A. M. A. Dias, J. C. Pàmies, J. A. P. Coutinho, I. M. Marrucho, L. F. Vega, SAFT Modeling of the Solubility of Gases in Perfluoroalkanes, *Journal of Physical Chemistry B* 108 (2004) 1450.

[51] J. C. Pàmies, L. F. Vega, Vapor-Liquid Equilibria and Critical Behavior of Heavy n-Alkanes Using Transferable Parameters from the Soft-SAFT Equation of State, *Industrial & Engineering Chemistry Research* 40 (2001) 2532.

[52] N. Pedrosa, J. C. Pàmies, J. A. P. Coutinho, I. M. Marrucho, L. F. Vega, Systematic Study of the Phase Equilibria of Ethylene Glycol Oligomers from a Molecular Modeling Approach, *Industrial & Engineering Chemistry Research* 44 (2005) 7027.

[53] N. Pedrosa, L. Vega, J. Coutinho, I. Marrucho, Phase Equilibria Calculations of Polyethylene Slutons from SAFT-Type Equations of State, *Macromolecules* 39 (2006) 4240.

[54] N. Pedrosa, L. F. Vega, J. A. P. Coutinho, I. M. Marrucho, Modeling the Phase Equilibria of Poly(ethylene glycol) Binary Mixtures with soft-SAFT EoS, *Industrial & Engineering Chemistry Research* 46 (2007) 4678.

[55] DIPPR, Design Institute for Physical Properties: DIPPR 801 database Brigham Young University (1998).

[56] A. M. A. Dias, H. Carrier, J. L. Daridon, J. C. Pàmies, L. F. Vega, J. A. P. Coutinho, I. M. Marrucho, Vapor - Liquid Equilibrium of Carbon Dioxide - Perfluoroalkane Mixtures: Experimental Data and SAFT Modeling, *Industrial & Engineering Chemistry Research* 45 (7) (2006) 2341.

[57] A. Dias, J. Pàmies, L. Vega, J. Coutinho, I. Marrucho, Modelling the solubility of gases in saturated and substituted perfluoroalkanes, *Polish Journal of Chemistry* 80 (2006) 143.

[58] F. Llovell, L. J. Florusse, C. J. Peters, L. F. Vega, Vapor-Liquid and Critical Behavior of Binary Systems of Hydrogen Chloride and n-Alkanes: Experimental Data and Soft-SAFT Modeling, *Journal of Physical Chemistry B* 111 (2007) 10180 .

[59] F. Eckert, A. Klamt, Validation of the COSMO-RS Method: Six Binary Systems, *Industrial & Engineering Chemistry Research* 40 (2001) 2371.

[60] A. Klamt, F. Eckert, COSMO-RS: a novel and efficient method for the a priori prediction of thermophysical data of liquids, *Fluid Phase Equilibria* 172 (2000) 43.

[61] A. Klamt, Prediction of the mutual solubilities of hydrocarbons and water with COSMO-RS, *Fluid Phase Equilibria* 206 (2003) 223.

[62] F. Eckert, A. Klamt, COSMOtherm. Version C2.1, Release 01.05, COSMOlogic GmbH & Co. Kg, Leverkusen, Germany, (2005).

[63] F. Eckert, COSMOtherm user's manual version C2.1, Release 01.05, COSMOlogic GmbH & Co. Kg: Leverkusen, Germany, (2005).

[64] M. G. Freire, L. M. N. B. F. Santos, I. M. Marrucho, J. A. P. Coutinho, Evaluation of COSMO-RS for the prediction of LLE and VLE of alcohols + ionic liquids, *Fluid Phase Equilibria* (article in press) (2007) .

[65] M. G. Freire, S. P. M. Ventura, L. M. N. B. F. Santos, I. M. Marrucho, J. A. P. Coutinho, Evaluation of COSMO-RS for the prediction of LLE and VLE of water and ionic liquids binary systems, *Brazilian Journal of Chemical Engineering* (2007) in press.

[66] N. M. D. Pedrosa. *Extension of the soft-SAFT Equation of State for Polymer Systems*. PhD Thesis, Departamento de Química, Universidade de Aveiro (2007).

[67] J. C. Pàmies. *Bulk and Interfacial Properties of Chain Fluids - A Molecular Modelling Approach*. PhD Thesis, Universitat Rovira i Virgili (2003).

[68] J. K. Johnson, J. A. Zollweg, K. E. Gubbins, The Lennard-Jones Equation of State, *Molecular Physics* 78 (1993) 591.

APPENDIX

Appendix A

Calibration of Pt100 temperature sensor

The Pt100 temperature sensor connected with a multimeter (HP 974A) was calibrated against a Platinum Resistance Thermometer (model 5613) with a thermometer Read Out (model 1521) from Fluke (Hart Scientific), which had been calibrated against a SPRT (25 ohm, Tinsley, 5187A) temperature probe using an ASL bridge model F26. The data for the calibration is presented in Table A.1.

Table A.1. Calibration of Pt100 temperature sensor.

T / ºC	R / Ω	T / ºC	R / Ω
0.00	101.98	80.00	132.59
20.00	109.66	95.00	138.36
40.00	117.34	125.00	149.67
60.00	124.99	150.00	159.02

The values of Table A.1 were correlated by a second order equation bellow:

$$T/ºC = 6.977119676\text{x}10^{-4}\ (R/\Omega)^2 + 2.445661037\ (R/\Omega) - 2.566134931\text{x}10^{2}$$

$$r^2 = 0.9999981467$$

The resistance was measured by the digital multimeter. The resistance values were taken manually and converted to the respective temperature values by means of the equation presented above.

Appendix B

Table B.1. LLE data of perfluoro-*n*-octane + *n*-octane system.

C_8F_{18} + C_8H_{18} (this work)				C_8F_{18} + C_8H_{18} (literature)[45]		
x_{PFC}	w_{PFC}	φ_{PFC}	T / K	x_{PFC}	φ_{PFC}	T / K
0.2733	0.5906	0.3646	349.1	0.0991	0.1437	334.24
0.4732	0.7750	0.5781	350.3	0.1669	0.2341	345.42
0.5366	0.8162	0.6385	349.2	0.2374	0.3220	349.06
0.6383	0.8712	0.7291	343.1	0.3013	0.3968	350.41
				0.4026	0.5069	350.32
				0.4984	0.6025	349.59
				0.5964	0.6927	346.02
				0.7245	0.8004	336.01
				0.7640	0.8316	327.71
				0.8919	0.9264	299.68

Table B.2. LLE data of PFMCH + toluene system.

C_7F_{14} + C_7H_8 (this work)				C_7F_{14} + C_7H_8 (literature)[13]		
x_{PFC}	w_{PFC}	φ_{PFC}	T ± σ[a] (K)	x_{PFC}	φ_{PFC}	T / K
0.0306	0.1070	0.0551	316.75 ± 0.11	0.057	0.101	336.9
0.0513	0.1705	0.0909	334.79 ± 0.07	0.120	0.201	356.3
0.1111	0.3220	0.1877	355.63 ± 0.20	0.190	0.302	360.9
0.2161	0.5116	0.3376	365.24 ± 0.03	0.267	0.402	362.1
0.2609	0.5728	0.3948	366.26 ± 0.02	0.353	0.502	361.8
0.3148	0.6358	0.4593	366.56 ± 0.07	0.450	0.602	360.4
0.3485	0.6703	0.4972	366.27 ± 0.05	0.560	0.702	355.2
0.4173	0.7313	0.5697	365.58 ± 0.07	0.686	0.802	341.9
0.5257	0.8081	0.6720	362.12 ± 0.03	0.831	0.901	316.0
0.6263	0.8643	0.7560	354.62 0.02			
0.7174	0.9060	0.8243	343.84 0.05			
0.8027	0.9392	0.8826	329.16 0.04			
0.8961	0.9704	0.9410	301.26 0.05			

[a] Standard deviation

Appendix C

In this Appendix a brief mathematical description of the soft-SAFT EoS will be made. For more detailed information on the terms used in soft-SAFT approach see references. [21, 66, 67]

The general expression of the soft-SAFT EOS is given in terms of the residual Helmholtz free energy per mole and can be written as a sum of contributions of several terms:

$$A^{res} = A^{total} - A^{ideal} = A^{ref} + A^{chain} + A^{assoc} + A^{polar} \qquad \text{(C.1)}$$

The ideal term form for mixtures is given by:

$$A^{ideal} = RT \sum_{i=1}^{n} (x_i \ln \rho_m^{(i)} \Lambda_i^3) - 1 \qquad \text{(C.2)}$$

The sum is over all species *i* of the mixture, $x_i = N_m(i)/N_m$ is the mole fraction, $\rho_m(i) = N_m(i)/V$ the molecular density, $N_m(i)$ the number of molecules, Λ_i the thermal de Broglie wavelength, and *V* the volume of the system.

The distinction of soft-SAFT among other SAFT-type equations is made by the reference term. The Lennard Jones EoS proposed by Johnson et al.[68], which is a modified Benedit-Webb-Rubbin EoS, was fitted with temperature dependent parameters (a_p, b_p and G_p) to simulation data.

$$A^{ref} = R\ \varepsilon \left(\sum_{p=1}^{8} \frac{a_p}{p} (\rho\ N_A\ \sigma^3)^p + \sum_{p=1}^{6} b_p G_p \right) \qquad \text{(C.3)}$$

The expression used to account for the formation of chains from m_i spherical monomers is

$$A^{chain} = R\,T \sum_{i=1}^{n} x_i (1 - m_i) \ln g_{LJ}^{(ii)}(\sigma_{ii}) \qquad \text{(C.4)}$$

where R is the ideal gas constant. The pair radial distribution function $g_{LJ}^{(ii)}(\sigma_{ii})$ of the reference fluid for the interaction of two segments in a mixture of segments, evaluated at the segment contact σ, provides structural information to the theory at the first-order level. This means that the model assumes conformality between branched and linear isomers of the same number of segments and also any information is considered about the attractive chain self-interaction beyond the formation of bonds.

The equation that represents the associative term is expressed as

$$A^{assoc} = R\,T \sum_i x_i \left[\sum_\alpha \left(\ln X_i^\alpha - \frac{X_i^\alpha}{2} \right) + \frac{M_i}{2} \right] \qquad \text{(C.5)}$$

where M_i is the number of association sites on each molecule of specie *i*, $\sum_\alpha$ represents a sum over all associating sites (on molecules of specie *i*) and X_i^α is the fraction of molecules *i* not bound to associating sites α, that is defined by

$$X_i^\alpha = \frac{1}{1 + N_A \rho \sum_j x_j \sum_\beta X_j^\beta \Delta^{\alpha_i \beta_j}} \qquad \text{(C.6)}$$

The variable $\Delta^{\alpha_i \beta_j}$ is the strength of the association bond and is given by:

$$\Delta^{\alpha_i \beta_j} = \int g_{LJ}^{ij}(12)\, f^{\alpha_i \beta_j}(12)\, d(12) \qquad \text{(C.7)}$$

with $g_{LJ}^{ij}(12)$ the pair distribution function of the reference fluid,

$f^{\alpha_i \beta_j}(12) = \exp(\varepsilon_{AB}^{HB} / k_B T) - 1$ is the Mayer function of the associating potential, and $d(12)$ denotes an unweighted average over all orientations and an integration over all separations of molecules 1 and 2.

In order to model mixtures, which may consist of chains with different number of segments, which in turn can be of different size and/or dispersive energy and, so, averaged parameters that simulate an “averaged” fluid that has the same thermodynamic properties as the mixture are used. Van der Waals’ mixing rules are in good agreement with molecular simulation data for spheres of similar size and the corresponding expressions for the size and energy parameters of the conformal fluid are:

$$\sigma^3 = \frac{\sum_i \sum_j x_i x_j m_i m_j \sigma_{ij}^3}{\left(\sum_i x_i m_i \right)^2} \tag{C.8}$$

$$\varepsilon \sigma^3 = \frac{\sum_i \sum_j x_i x_j m_i m_j \varepsilon_{ij} \sigma_{ij}^3}{\left(\sum_i x_i m_i \right)^2} \tag{C.9}$$

The expressions C.8 and C.9 involve the mole fraction x_i and the chain length m_i of each of the components of the mixture of chains, denoted by the indices *i* and *j*, and the unlike ($j \neq i$) interaction parameters σ_{ij} and ε_{ij}, which are determined by means of combination rules. The Lorentz-Berthelot combining rules are commonly used and were also employed in this work

$$\sigma_{ij} = \eta_{ij} \frac{\sigma_{ii} + \sigma_{jj}}{2} \tag{C.10}$$

$$\varepsilon_{ij} = \xi_{ij} \sqrt{\varepsilon_{ii} \varepsilon_{jj}} \tag{C.11}$$

where the factors η_{ij} and ξ_{ij} modify the arithmetic and geometric averages, respectively, between components *i* and *j*.

A polar term may be included to account for electrostatic contribution for the thermodynamic properties of a system where at least one of the components has a quadrupole moment. The Helmholtz free energy in terms of the perturbed quadrupole-quadrupole potential with the Padé approximation can be written as:

$$A^{polar} = A^{qq} = A_2^{qq}\left(\frac{1}{1-\frac{A_3^{qq}}{A_2^{qq}}}\right) \tag{C.12}$$

The expressions for A2 and A3, the second and third order perturbation terms, are defined as

$$A_2^{qq} = \frac{-14\pi N\rho}{5k_BT}\sum_i\sum_j x_i x_j \frac{Q_i^2 Q_j^2}{\sigma_{ij}^7} J_{ij}^{(10)} \tag{C.13}$$

$$A_3^{qq} = \frac{-144\pi N\rho}{245(k_BT)^2}\sum_i\sum_j x_i x_j \frac{Q_i^3 Q_j^3}{\sigma_{ij}^{12}} J_{ij}^{(15)} \tag{C.14}$$

The term *J* runs over two and three molecule correlation functions for the reference fluid. The integrals were calculated using molecular dynamics data for a pure Lennard-Jones fluid and the resulting values were fitted to simple functions of temperature and density.

$$|J^{(n)}| = A_n\rho^2\ln T + B_n\rho^2 + C_n\rho\ln T + D_n\rho + E_n\ln T + F_n \tag{C.15}$$